ARTICLE

Microglia and their LAG3 checkpoint underlie the antidepressant and neurogenesis-enhancing effects of electroconvulsive stimulation

Neta Rimmerman[1], Hodaya Verdiger[1], Hagar Goldenberg[1], Lior Naggan[1], Elad Robinson[1], Ewa Kozela[1], Sivan Gelb[2], Ronen Reshef[1], Karen M. Ryan[3,4], Lily Ayoun[1], Ron Refaeli[5], Einat Ashkenazi[1], Nofar Schottlender[1], Laura Ben Hemo-Cohen[1], Claudia Pienica[1], Maayan Aharonian[1], Eyal Dinur[1], Koby Lazar[1], Declan M. McLoughlin[3,4], Ayal Ben Zvi[2] and Raz Yirmiya[1]✉

Despite evidence implicating microglia in the etiology and pathophysiology of major depression, there is paucity of information regarding the contribution of microglia-dependent molecular pathways to antidepressant procedures. In this study, we investigated the role of microglia in a mouse model of depression (chronic unpredictable stress—CUS) and its reversal by electroconvulsive stimulation (ECS), by examining the effects of microglia depletion with the colony stimulating factor-1 antagonist PLX5622. Microglia depletion did not change basal behavioral measures or the responsiveness to CUS, but it completely abrogated the therapeutic effects of ECS on depressive-like behavior and neurogenesis impairment. Treatment with the microglia inhibitor minocycline concurrently with ECS also diminished the antidepressant and pro-neurogenesis effects of ECS. Hippocampal RNA-Seq analysis revealed that ECS significantly increased the expression of genes related to neurogenesis and dopamine signaling, while reducing the expression of several immune checkpoint genes, particularly lymphocyte-activating gene-3 (*Lag3)*, which was the only microglial transcript significantly altered by ECS. None of these molecular changes occurred in microglia-depleted mice. Immunohistochemical analyses showed that ECS reversed the CUS-induced changes in microglial morphology and elevation in microglial LAG3 receptor expression. Consistently, either acute or chronic systemic administration of a LAG3 monoclonal antibody, which readily penetrated into the brain parenchyma and was found to serve as a direct checkpoint blocker in BV2 microglia cultures, rapidly rescued the CUS-induced microglial alterations, depressive-like symptoms, and neurogenesis impairment. These findings suggest that brain microglial LAG3 represents a promising target for novel antidepressant therapeutics.

Molecular Psychiatry (2022) 27:1120–1135; https://doi.org/10.1038/s41380-021-01338-0

INTRODUCTION

Despite recent progress in the understanding of the molecular, cellular and circuit-level correlates of depression, the biological mechanisms that causally underlie this disease are still unclear. Similarly, the mechanisms of action of antidepressant procedures, including antidepressant drugs and electroconvulsive therapy (ECT), are not fully elucidated [1, 2]. Over the past two decades, ample evidence has accumulated showing that inflammatory processes play an important role in the etiology and pathophysiology of major depression [3–7]. Moreover, anti-inflammatory effects constitute an important mechanism of action of antidepressant drugs, particularly in patients demonstrating elevated levels of inflammatory markers before treatment [8]. Conversely, several lines of evidence support the notion that under certain conditions depression can be associated with suppression, rather than activation of inflammatory processes [9–11]. For example, antidepressants often provide clinical relief without attenuating pro-inflammatory markers [12]. Moreover, antidepressants can sometimes increase the production of pro-inflammatory cytokines [13, 14], whereas non-steroidal anti-inflammatory drugs can attenuate the anti-depressant effects of selective serotonin reuptake inhibitors (SSRIs). Furthermore, treatment with anti-inflammatory drugs, which is effective in patients with high levels of baseline peripheral inflammatory markers or a central marker of microglial activation (assessed by positron emission tomography (PET) imaging of the TSPO ligand), has no effects on patients with low levels of baseline inflammation and microglia activation, and can even exacerbate depression in some of these patients [15–20].

A particularly important development has been the realization that brain microglia cells may be causally involved in the development of depression [21–23]. The role of microglia in depression is complex, given that some studies indicate that depression is associated with microglia activation, whereas others suggest it is associated with microglia decline and degeneration. Accordingly, we have previously suggested that any extreme deviation from the normal microglial homeostatic activation status (i.e., either hyper- or hypo-activation) contributes to the development of depression [21], as evidenced by

[1]Department of Psychology, The Hebrew University of Jerusalem, Jerusalem, Israel. [2]Department of Developmental Biology and Cancer Research, The Institute for Medical Research Israel-Canada, Faculty of Medicine, Hebrew University of Jerusalem, Jerusalem, Israel. [3]Trinity College Institute of Neuroscience, Trinity College Dublin, Dublin, Ireland. [4]Department of Psychiatry, Trinity College Dublin, St. Patrick's University Hospital, James Street, Dublin, Ireland. [5]Edmond & Lily Safra Center for Brain Sciences, The Hebrew University of Jerusalem, Jerusalem, Israel. ✉email: razyirmiya@huji.ac.il

Received: 17 March 2021 Revised: 16 September 2021 Accepted: 1 October 2021
Published online: 14 October 2021

the following: (1) Microglia in depressed patients exhibit abnormal morphology, distribution and cytokine production (assessed in post-mortem studies) [24–27] and activation status (assessed by PET imaging) [3, 16, 28–31]. Evidence of both hyper- and hypo-activation microglial phenotypes were obtained in these studies. Furthermore, in a recent study, the status of microglia activation was associated with the efficacy of a microglia-suppressive drug treatment [16]. (2) Genetic variants in microglia-relevant genes influence the development of depression [32]. (3) In RNA-Seq studies of brain tissues from depressed patients, the main finding was lower expression in molecular pathways involved in microglial and immune system regulation [33, 34]. (4) Antidepressant drugs modulate microglial activation status [35]. (5) Altered expression of specific microglial genes in mice, particularly *CX3CR1*, induce stress resilience and prevents the development of chronic stress-induced depression [36–38]. (6) Microglia are important regulators of adult neurogenesis [39–41], which in turn modulates the development of depression and constitutes a major target for antidepressant therapies [42, 43]. (7) In animal models of stress-induced depression, microglia in several stress-responsive brain areas exhibit morphological and functional markers of activation, which underlie at least some of the neurobehavioral symptoms [44–49]. On the other hand, in mice exposed to a specific regimen of chronic unpredictable stress (CUS), an initial period of stress-induced microglial proliferation and activation leads to subsequent microglial apoptosis, decline in density, and assumption of dystrophic morphology. Furthermore, treatment of "depressed-like" mice in this model with microglia-stimulating drugs (including lipopolysaccharide (LPS), macrophage colony-stimulating factor (M-CSF) or granulocyte-macrophage colony-stimulating factor (GM-CSF)), completely reversed the depressive-like symptoms, in association with dramatic increases in hippocampal neurogenesis [50–52]. Similar microglia-suppressive effects have been described in several other animal models of depression, including chronic social defeat stress, chronic restraint stress [50], early social isolation [53], and adult social isolation [44]. Consistent with these findings, microglia suppressive drugs, including minocycline or IL-1 receptor antagonist, which produce antidepressant effects in treatment-resistant depressed patients or in "depressed-like" mice with a high inflammatory/microglial status [15, 54–56], had no beneficial effect in a depression model associated with microglial decline [52]. Together, these findings suggest that deviations from the microglial homeostasis status should be regarded as important therapeutic targets for major depression, and restoration of microglial homeostasis may constitute the mechanism of action of some currently used antidepressant procedures.

To further test this hypothesis, we examined the effects of microglia manipulations in mice on normal mood-related behavior, as well as on CUS-induced depressive-like symptoms, and their amelioration by an antidepressant procedure. We particularly focused on electroconvulsive stimulation (ECS), the animal model equivalent of ECT, which is considered one of the most effective antidepressant procedures [57]. ESC has been previously found to produce alterations in microglial physiology under various conditions [58–60], including the induction of microglia activation in non-stressed [61] and chronically stressed [62] mice. Furthermore, we elucidated the cellular and molecular mechanisms that underlie the microglia-dependent antidepressant effects of ECS, discovering a particularly important role for the microglial checkpoint receptor lymphocyte-activation gene-3 (LAG3).

RESULTS

Microglia depletion does not induce depressive-like or other behavioral symptoms

Environmental, pharmacological, or genetic manipulations that modulate microglia dynamics have been shown to affect emotional coping with stress and regulate mood [21, 63, 64]. However, the role of microglia in maintaining emotionality and mood under normal quiescent conditions has not been directly explored. In the present experiment, we used a non-invasive pharmacological treatment with a diet containing the colony stimulating factor (CSF)-1 receptor antagonist PLX5622 (PLX) to induce whole-brain microglia depletion [65]. After 3 weeks on the PLX diet, mice exhibited marked reduction in the number of microglia in the hippocampus (Figs. 1a, 1b) and in all other regions of the brain [40], as compared with a control diet (CDiet). Despite the microglia depletion, there were no differences between the groups in body weight (Fig. 1c), sucrose preference (Fig. 1d), social exploration (SE; Fig. 1e), spatial hippocampus-dependent memory functioning (Fig. 1f), levels of anxiety (time spent in the open arms of the elevated plus maze) (Fig. 1h), or locomotor activity in the elevated plus maze (Fig. 1g).

Microglia depletion or suppression abrogates the antidepressant and neurogenesis-promoting effects of ECS

We next examined the involvement of microglia in the development of depressive-like behavior, and its reversal by ECS, which was previously reported to affect microglial morphology and activation status [60–62, 66] (Fig. 2a). Similar to the results of the first experiment, the non-stressed PLX-treated group showed normal hedonic behavior (sucrose preference), SE levels, and immobility in the Porsolt forced swim test (FST; Fig. 2b,d,f), demonstrating that whole brain microglia depletion (even for an extended period of more than 9 weeks of continuous depletion) alone did not induce depressive-like behavior. Furthermore, following CUS exposure, mice from both the CDiet and PLX groups displayed similar reductions in sucrose preference and SE (Fig. 2b,d).

Microglia depletion markedly attenuated the anti-depressant effects of ECS. Specifically, although ECS increased sucrose preference in all CUS-exposed groups, this increase was significantly greater in the CDiet group (in which ECS restored sucrose preference to the normal levels usually observed in non-stressed mice) than in the PLX-treated group (Fig. 2c). A similar pattern of results was observed in the SE test, but these findings did not reach statistical significance (Fig. 2e). In the FST, conducted at the completion of the ECS regimen, PLX alone produced no effect, demonstrating that the mere lack of microglia does not produce despair. However, the effect of ECS in reducing immobility time was significantly smaller in the PLX-treated compared to the CDiet-treated group (Fig. 2f), verifying the crucial involvement of microglia in the antidepressant mechanism of ECS. Immunohistochemical analysis of hippocampal neurogenesis demonstrated the juxtaposition of microglia and doublecortin (DCX)-labeled newborn neurons, suggesting a physical basis for their interactions (Supplementary Video 1 and 2). In CUS-exposed mice treated with CDiet, ECS significantly elevated the number of DCX-labeled newborn neurons in the dentate gyrus (compared with sham-stimulation (SHAM)-treated mice) up to the levels observed in non-stressed mice (Fig. 2g–i). In contrast, in CUS-exposed mice treated with PLX, ECS caused the opposite effect, producing a significant decrease (compared with SHAM-treated mice) in the number of DCX-labeled newborn neurons in the dentate gyrus (Fig. 2g, j, k).

To further examine the role of microglia in the therapeutic effect of ECS, we examined the effects of minocycline (MINO), an established pharmacological blocker of microglia activation [67], on the anti-depressant and neurogenesis-promoting effects of ECS. Five weeks after the initiation of CUS exposure, mice were treated with either SHAM stimulation or ECS for 2.5 weeks, concurrently with continuous administration of MINO (via the drinking water) or water (WAT) only (Fig. 2l). Compared with non-stress controls, WAT-drinking CUS-exposed mice that were SHAM treated displayed a significant reduction in sucrose preference, which was reversed by ECS (Fig. 2m). In contrast, in MINO-drinking mice ECS had no beneficial effect. In the FST, ECS reduced immobility time in both WAT-drinking controls and MINO-treated

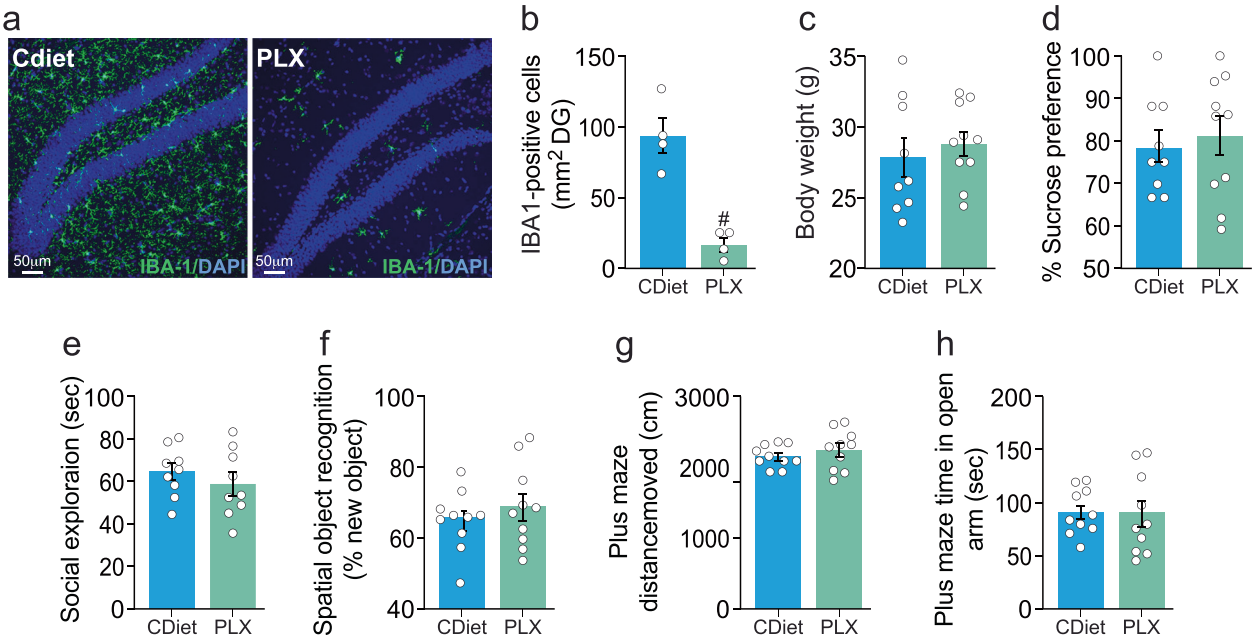

Fig. 1 Effects of microglia depletion on body weight and behavior. a Representative fluorescent micrographs of IBA-1-labled microglia (green) in the hippocampal dentate gyrus (DG) of normal WT mice treated with either a control diet (CDiet) or PLX-containing diet for 3 weeks (blue=Dapi). **b** Mice exposed to the PLX diet had a significantly lower number of hippocampal dentate gyrus (DG) microglia (reduction of 80%) than CDiet-exposed mice ($t_6 = 5.760$, $p < 0.001^{\#}$, $n = 4$ mice/group). Normal mice treated with either PLX or CDiet for 3 weeks showed no differences in **c** body weight, **d** sucrose preference, **e** social exploration (SE), **f** spatial hippocampus-dependent memory in the object recognition task, **g** activity levels (distance moved in the elevated plus maze, or **h** anxiety levels (time spent in the open arms of an elevated plus maze); $p > 0.1$, $n = 8$–10 per group).

mice (Fig. 2n). Although this reduction was somewhat smaller in the MINO-treated mice, the differential effect of ECS in the WAT and MINO conditions did not reach statistical significance. MINO alone produced no effects in the Sucrose Preference and the FST; this finding is expected, as previous studies in which MINO was found to exert antidepressant effects [15, 68, 69] probably included mainly subjects with microglia activation [49, 56, 70], whereas the current experiment was based on a depression model associated with microglia suppression [52]. Thus, MINO could not influence the already declined microglia status, while reversing the changes in this status induced by ECS. Assessment of neurogenesis in the dentate gyrus (DG) by counting DCX- positive cells after treatment termination revealed that as expected, CUS significantly reduced the levels of neurogenesis in the WAT- and MINO-drinking SHAM-treated groups (compared with control, non-stressed mice). In the WAT-drinking group, ECS reversed the deleterious effect of CUS, elevating the levels of neurogenesis to those of non-stressed controls. In contrast, in the MINO-drinking group, the beneficial effect of ECS on neurogenesis was completely blocked, corroborating the critical role of microglia activation in ECS-induced neurogenesis promotion (Fig. 5o).

Microglia depletion blocks ECS-induced molecular alterations

To elucidate the potential molecular mechanisms underlying the attenuated anti-depressant efficiency of ECS in PLX-treated mice, we explored differences in gene expression in the hippocampus, which is involved in the regulation of emotional and cognitive processes as well as in mediating the therapeutic effects of ECT [71]. In CUS-exposed mice, RNA sequencing (RNA-Seq) analysis revealed a marked effect of the PLX treatment on hippocampal gene expression, likely reflecting the consequences of microglial depletion. In SHAM-treated mice specifically, a total of 390 genes were differentially regulated in PLX- vs. CDiet-treated mice, of which 338 genes were down-regulated and 52 were up-regulated ($q < 0.32$, with a cutoff of ±1.3 fold change). In ECS-treated mice, a total of 497 genes were differentially regulated in PLX vs. CDiet-treated mice, of which 384 genes were down-regulated and 113 were up-regulated ($q < 0.32$, with a cutoff of ±1.3 fold change) (see GEO Series accession number GSE123027). The RNA-Seq analysis also revealed that the expression of several hippocampal genes was significantly modulated by ECS. In CDiet mice specifically, a total of 15 genes were differentially expressed between the CUS-exposed SHAM vs. ECS mice, out of which nine genes were down-regulated and 6 were up-regulated (Fig. 3a; $q < 0.32$, with a cutoff of ±1.3 fold change). Six of the down-regulated genes were previously shown to influence immune processes, half of them, including lymphocyte-activation gene 3 (*Lag3*), cluster of differentiation 180 (*Cd180*, also known as *Rp105*) and tryptophan 2,3-dioxygenase (*Tdo2*) serve as immune checkpoints. The expression of two additional immune checkpoints, cluster of differentiation 86 (also termed *B7-2*) and programmed death-ligand 1 (*Pd-L1*), were also decreased by ECS but their significance level did not reach the correction (q) cutoff (Supplementary Table 1). The genes whose expression was up-regulated by ECS included *Sox11*, which is critical for neurogenesis, as well as dopamine receptor D1 (*Drd1*) and synaptic vesicle glycoprotein 2C, which mediate dopaminergic neurotransmission. Remarkably, in the PLX-treated groups no genes were differentially expressed between CUS-exposed SHAM and ECS mice.

In order to validate the RNA-Seq data, we conducted real time quantitative PCR experiments, assessing the expression of selected genes that were significantly changed by PLX or ECS in the hippocampus of CUS-exposed mice (Fig. 3). The housekeeping gene glyceraldehyde-3-phosphate dehydrogenase (*Gapdh)* was used as a reference to all measured gene transcripts. Consistent with the results of the RNA-Seq analysis, transcripts of microglial genes, such as *Iba1 and P2ry12* (Fig. 3b,c), were significantly decreased in the PLX-treated mice, regardless of ECS treatment. The expression of only two genes that were significantly decreased by the PLX diet in the RNA-Seq analysis, *Lag3* and *Cd180* (Fig. 3a), were also found to be reduced by ECS. Validation by qPCR verified that in CDiet-treated mice *Lag3* expression was

significantly reduced in ECS compared to SHAM-treated mice (Fig. 3d). A similar trend was observed for *Cd180* expression, but this result did not reach statistical significance (Fig. 3e). We also validated the findings of the RNA-Seq analysis regarding four gene transcripts (*Tdo2, Pla2g4e, Sox11, and Drd1* (Fig. 3f–i)), that were not affected by microglia depletion but were significantly altered by ECS in the CDiet treated mice. Specifically, the qPCR analysis verified that the expression of the tryptophan 2,3-dioxygenase (*Tdo2*) gene, which was previously found to be involved in depression and the mechanism of action of antidepressants [5, 7, 72, 73], as well as the phospholipase A2 group IVE (*Pla2g4e) gene*, which is involved in the synthesis of endocannabinoids [74],

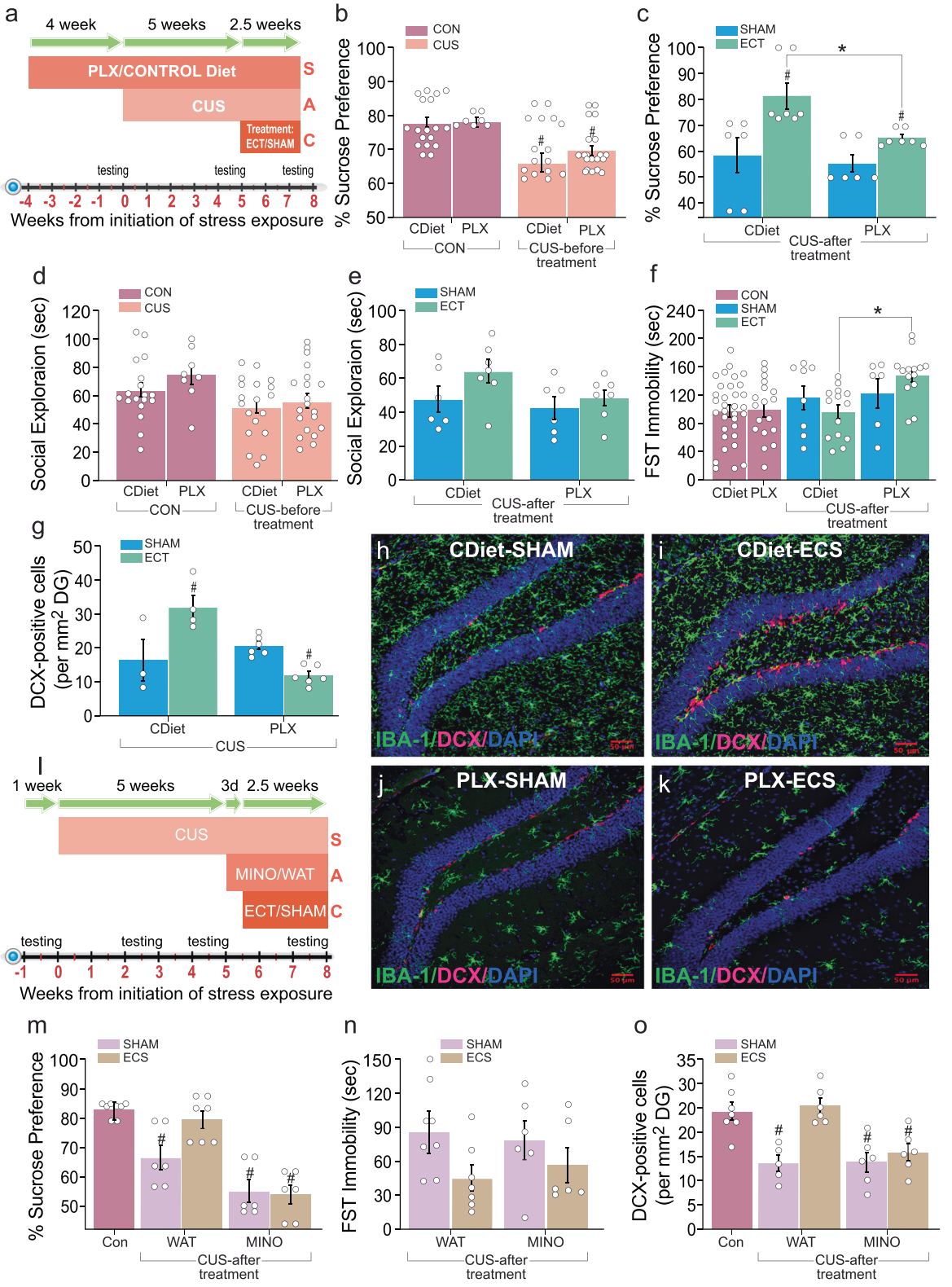

Fig. 2 Involvement of microglia in the antidepressant and neurogenesis-enhancing effects of ECS. a Timeline of the experiment. Following 4 weeks' consumption of either a PLX-containing diet (PLX) or CDiet, mice were exposed to 5 weeks of CUS or left undisturbed in their home cage (no-stress control (CON) condition). After assessment of hedonic, social, and emotional behavior, mice in the CUS-exposed groups were further divided into two sub-groups, administered with either ECS (three-times per week for 2.5 weeks) or sham stimulation (SHAM). After the treatment, mice were tested again in the sucrose preference, SE and Porsolt forced swim test (FST), and then sacrificed (SAC) for histological analyses. **b** Mice treated with CDiet or PLX displayed similar levels of sucrose preference under the CON condition as well as a similar CUS-induced reduction in sucrose preference, reflected by a significant main effect of CUS ($F_{1,60} = 21.433$, $p < 0.0001$; $p < 0.01^{\#}$ compared with the corresponding CON group) ($n = 8$–20 per group). **c** Microglia depletion attenuated the effects of ECS on CUS-induced reduction in sucrose preference, reflected by significant main effects of ECS ($F_{1,22} = 13.925$, $p < 0.001$) ($n = 6$–7/group), and PLX (($F_{1,22} = 4.699$, $p < 0.05$; $p < 0.05^{\#}$ compared with the corresponding SHAM group; $p < 0.05^{*}$ between CDiet-ECS and PLX-ECS groups) ($n = 6$–7/group). **d** Mice treated with the CDiet or PLX displayed similar levels of SE, as well as a similar CUS-induced reduction in SE, reflected by a significant main effect of CUS ($F_{1,64} = 6.993$, $p < 0.01$) ($n = 8$–20/group). **e** ECS produced only a trend towards increased SE in the CDiet-treated group ($n = 6$–7/group), but this difference did not reach statistical significance. **f** In non-stressed CON mice, the levels of immobility in the FST were similar in the CDiet and PLX groups, whereas in CUS-exposed mice, ECS exposure differentially modulated the immobility time, reflected by a significant difference among the groups ($F_{1,87} = 3.56$, $p < 0.01$) ($n = 6$–11/group). Specifically, following ECS, mice exposed to the CDiet displayed significantly lower forced swim immobility than mice exposed to PLX ($p < 0.001^{*}$), reflecting the abrogation of the antidepressant effect of ECS in microglia-depleted mice. **g** CUS-exposed mice treated with either CDiet or PLX displayed similar levels of neurogenesis (number of DCX-labeled cells per mm^2 of the hippocampal DG). However, while ECS significantly increased DG neurogenesis in the CUS-exposed CDiet mice, it significantly reduced neurogenesis in the microglia-depleted mice. This was reflected by a significant diet by stress interaction (($F_{1,87} = 20.1$, $p < 0.001$; $p < 0.005^{\#}$ compared with the corresponding SHAM-treated group) ($n = 3$–6/group). Representative pictures of IBA-1-labled microglia (green) and DCX-labeled newborn neurons (red) in the DG of SHAM-treated **h** or ECS-treated **i** depressed-like mice consuming the CDiet, as well as SHAM-treated **j** or ECS-treated **k** depressed-like mice consuming the PLX diet. All nuclei were labeled blue (Dapi). **l** Time line of the experiment. Following 5 weeks exposure to CUS or to a non-stress control (CON) period, and verification of CUS-induced depressive-like symptoms, half of the CUS-exposed mice were initiated on minocycline (MINO; administered in the drinking water)) and the other half on water (WAT) only. After 3 days, half of the mice in each of the WAT/MINO groups were further divided into two sub-groups and administered with either ECS (three-times per week for 2.5 weeks) or SHAM treatment. **m** CUS-exposed mice displayed differential treatment-dependent responsiveness to ECS in the sucrose preference test ($F_{4,\ 28} = 5.96$, $p < 0.001$, $n = 6$–7 per group). Post-hoc analysis revealed that ECS induced a significant increase in sucrose preference in WAT-drinking mice, but not in MINO-treated mice ($p < 0.05^{\#}$ compared with the control and the ECS-treated water-drinking groups). **n** In the FST, ECS produced an overall reduction in immobility time ($F_{1,21} = 4.33$ $p < 0.05$, $n = 6$–7 per group). Post-hoc analysis trended towards a significant difference between the SHAM and ECS conditions within the WAT-drinking mice ($p = 0.079$), but not the MINO-treated mice. **o** Compared with CON mice, CUS-exposed mice that received SHAM stimulation, concurrently with either WAT or MINO administration, displayed lower levels of neurogenesis. ECS reversed the effect of CUS in WAT drinking CUS mice, but it had no effects in CUS mice concurrently treated with MINO. This was reflected by a significant overall group difference in DCX-positive cell density ($F_{4,25} = 5.29$, $p < 0.005$; $p < 0.01^{\#}$ compared with either the non-stressed control or the WAT-drinking ECS-treated groups ($n = 5$–7 brains/condition).

were significantly down-regulated by ECS in the CDiet but not in the PLX-treated group. Furthermore, the expression levels of *Sox11*, a gene associated with adult neurogenesis [75], and the dopamine receptor 1 (*Drd1)* gene, which is also associated with neurogenesis [76] as well as regulation of brain-derived neurotrophic factor production [77]), were significantly increased by ECS in the CDiet but not the PLX-treated group.

ECS modulates microglial density, morphology, and LAG3 expression

We previously showed that exposure to the specific CUS paradigm utilized here reduces the number and alters the morphology of microglia in the hippocampal DG but not necessarily in other brain regions [52]. Furthermore, microglia within the DG exhibit unique properties that support their role in adult hippocampal neurogenesis [78]. Therefore, to elucidate the effects of ECS on microglia in this model, we analyzed the morphometric changes in DG microglia of mice exposed to 5 weeks of CUS followed by 2.5 weeks of either ECS or SHAM treatment. We found that compared with the non-stress control group, the DG microglial density was significantly reduced in CUS-exposed SHAM-treated mice; but this reduction was reversed by ECS (Fig. 4a). Microglial IBA1-positive soma size was significantly increased in the CUS-exposed ECS-treated group compared to both the non-stress control and CUS-exposed SHAM-treated groups (Fig. 4b). Compared with the non-stress control group, the total area of DG microglia (which includes the processes area) was significantly reduced in CUS-exposed SHAM-treated mice, but this reduction was reversed by ECS (Fig. 4c). Finally, the total length of microglial IBA1-immunostained processes in the DG of CUS-exposed mice was significantly reduced in the CUS-exposed mice compared to non-stressed controls (Fig. 4d) with no effect of ECS on this parameter. Overall, the ECS-induced reversal of CUS-induced decreases in microglia number and cell size represents a normalization of microglia activation status, while the increase in soma area and decrease in the length of processes are indicative of a mild activated state (Fig. 4e–g).

LAG3 belongs to the immunoglobulin (Ig) superfamily expressed by many immune cells, including brain microglia [79–81]. Lag3 contains an MHC-II interacting domain and a KIEELE motif, allowing it to negatively regulate T cell expansion and homeostasis [82]. Of note, so far, little is known about the inhibitory immune checkpoint activity of microglial LAG3 in the brain. Our RNA-Seq analysis revealed a marked reduction of *Lag3* expression in PLX-treated mice. Furthermore, *Lag3* was the microglial gene that was most robustly reduced by ECS in the RNA-Seq and qPCR analyses (Fig. 3a, d). However, the cellular localization of brain LAG3 has never been examined. Immunohistochemical staining with IBA-1 and LAG3 antibodies revealed that LAG3 protein in the brain is strongly expressed by microglia. Specifically, all IBA-1-labeled microglia were co-labeled with LAG3, the staining of which was also observed in association with blood vessels (Fig. 4h-j). Consistently with the findings of the molecular analyses (Fig. 3a, d), in PLX-treated mice the remaining microglia expressed much less LAG3 (although expression by blood vessels-associated cells remained intact) (Fig. 4k–m). Examination of individual cells demonstrated that LAG3 was expressed on the microglial cell soma and processes (Fig. 4n–p). In sections from the frontal cortex of humans, P2Y12-labeled microglia were also shown to express LAG3 (Fig. 4q–s).

Measurements of the intensity of microglial LAG3 staining (in soma and processes), revealed that in CUS-exposed ("depressed-like") mice receiving SHAM treatment, the intensity was significantly elevated compared with naïve controls (Fig. 4t, u, v). This elevation in a microglial checkpoint molecule is a possible contributor to the CUS-induced microglia decline that we previously reported [52] and verified in the present study. ECS reduced the intensity of LAG3 protein in microglia (Fig. 4t, v, w), in

line with the effects of ECS on *Lag3* mRNA (Fig. 3a,d). This reduction corroborates our findings regarding the effects of ECS on the number and morphology of microglia, suggesting that ECS-induced decrease in LAG3 checkpoint contributes to the consequent morphological changes.

Blockade of microglial LAG3 checkpoint with a specific anti-LAG3 monoclonal antibody induces antidepressant and neurogenesis-enhancing effects

The signaling pathway of LAG3 in the brain is not well characterized. As an established immune checkpoint receptor, LAG3 probably

a *Genes significantly differentially expressed in ECT versus SHAM in control diet CUS-exposed mice*

Gene Symbol	Gene Name	Log Ratio	p-value	False Discovery Rate (q-value)
Immune checkpoint				
Lag3	lymphocyte activating gene 3	-1.831	0.000745	0.319
Cd180	CD180 molecule	-1.613	0.000858	0.319
Tdo2	tryptophan 2,3-dioxygenase	-1.471	0.000123	0.137
Immune system-related				
Csf2rb2	colony stimulating factor 2 receptor beta common subunit	-1.834	2.34E-7	0.002
H2-D1	major histocompatibility complex, class I, A	-1.408	0.000785	0.319
B2m	Beta-2 microglobulin	-1.322	0.000234	0.173
Endocannabinoid signaling				
Pla2g4e	phospholipase A2 group IVE	-1.554	0.000741	0.319
Transcription factors				
Zcchc5	zinc finger CCHC-type containing 5	-1.725	0.000059	0.0987
Mafa	MAF bZIP transcription factor A	-1.695	0.000203	0.173
Neurogenesis				
Sox11	SRY-box 11	1.434	5.51E-9	0.00011
Synaptic neurotransmission				
Drd1	dopamine receptor D1	1.483	0.000232	0.173
Sv2c	synaptic vesicle glycoprotein 2C	1.42	0.000166	0.157
Other				
Noxred1	NADP dependent oxidoreductase domain containing 1	1.979	0.000927	0.319
Serinc2	serine incorporator 2	1.54	0.000589	0.294
Pdia4	protein disulfide isomerase family A member 4	1.442	0.000569	0.294

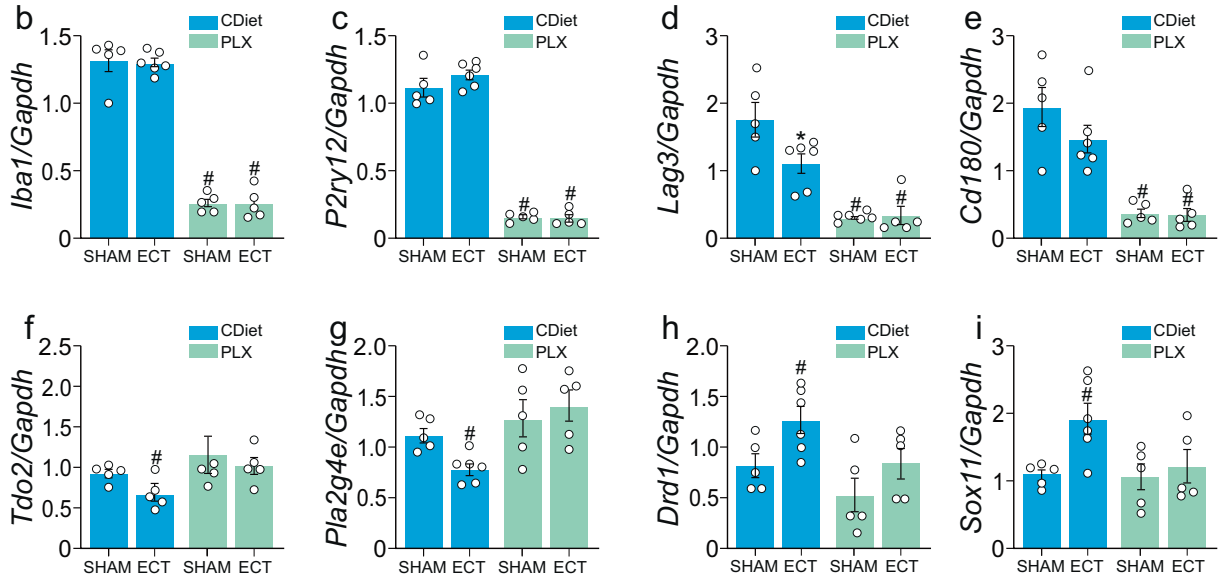

Fig. 3 ECS-induced molecular changes are abrogated in microglia-depleted mice. a RNA-Seq analysis showed that compared with SHAM-treated CUS-exposed mice, ECS significantly reduced the expression of several immune checkpoint and other immune-related genes as well as genes related to the endocannabinoid system and transcription regulation, but increased the expression of genes related to dopaminergic neurotransmission, neurogenesis, and other processes. These findings only appeared in CDiet-treated mice, whereas none of the ECS-induced molecular changes occurred in PLX-treated mice. Validation by qPCR of the expression of selected genes showing significant diet (PLX, CDiet) or antidepressant treatment (SHAM, ECS) effects in the RNA-seq analysis. **b** *Iba1* and **c** *P2ry12* gene expression validation revealed a main effect of diet ($F_{1,17} = 436.0$ and $F_{1,17} = 625.8$, respectively, $p < 0.001$; $p < 0.0001^{\#}$ compared with the corresponding CDiet group; $n = 5$–6/condition, for this and for all other validations presented in this figure). **d** *Lag3* gene expression validation revealed a main effect of diet ($F_{1,17} = 46.8$ $p < 0.001$; $p < 0.0001^{\#}$ compared with the corresponding CDiet group). In addition, there was a significant interaction between diet and treatment ($F_{1,17} = 4.43$, $p < 0.05$; $p < 0.02^{*}$ compared with the CDiet-SHAM-treated group). **e** *Cd180* gene expression validation revealed a main effect of Diet ($F_{1,17} = 47.3$, $P < 0.001$; $p < 0.0001^{\#}$ compared with the corresponding CDiet group). **f** *Tdo2* gene expression validation revealed a significant main effect of diet ($F_{1,16} = 4.6$, $p < 0.05$; $p < 0.05^{\#}$ compared with the CDiet-SHAM-treated group). **g** Pla2g4e gene expression validation revealed a main effect of diet ($F_{1,17} = 10.44$, $p < 0.01$; $p < 0.01^{\#}$ compared with the CDiet-SHAM-treated group). **h** *Drd1* gene expression validation revealed a main effect of Diet ($F_{1,17} = 6.14$, $p < 0.05$) and a main effect of treatment ($F_{1,16} = 7.08$, $p < 0.05$; $p < 0.05^{\#}$ compared with the CDiet-SHAM-treated group). **i** *Sox11* gene expression validation revealed a main effect of treatment ($F_{1,16} = 5.927$ $p < 0.05$; $p < 0.05^{\#}$ compared with the CDiet-SHAM-treated group).

delivers inhibitory signals to control brain immune cell homeostasis. Specific antibodies to LAG3 have been shown to serve as immune checkpoint blockers, which stimulate peripheral immunity and confer anti-tumor resistance [83]. Additionally, similar to other immune cells, microglia responses are also tightly regulated by various checkpoint molecules [84]. Therefore, we sought to determine whether inhibition of the LAG3 microglial checkpoint with a specific anti-LAG3 monoclonal antibody (mAb) can induce ECS-like beneficial effects on depression and neurogenesis. Following 5 weeks of CUS exposure, mice were acutely injected (i.p.) with either an anti-LAG3 mAb (100 µg of LEAF™ Purified anti-mouse CD223, Biolegend), or an isotype IgG control antibody. Sucrose preference and immobility in the FST were assessed three and 5 days later, respectively, after which all animals were sacrificed (SAC) (Fig. 5a). Compared with their pre-treatment levels, CUS-exposed IgG antibody-treated mice did not exhibit any change in sucrose preference after treatment. In contrast, mice treated with the anti-LAG3 mAb displayed a complete reversal of the pre-treatment CUS-induced reduction in sucrose preference (Fig. 5b). Immobility in the forced-swim test at 5 days post-treatment was significantly higher in CUS-exposed mice treated with IgG antibodies (as compared with non-stressed IgG-treated mice). This effect of CUS on despair in the FST was rescued by treatment with the anti-LAG3 mAb (Fig. 5c). These findings suggest that anti-LAG3 treatment can serve as a fast-acting antidepressant procedure. Analysis of the treatment effects on microglial morphology demonstrated that whereas LAG mAb treatment had no effect on total microglia size (Fig. 5d), it completely reversed the CUS-induced reduction in microglial process numbers (Fig. 5e), with a similar, albeit not significant, effect on processes length (Fig. 5f). CUS exposure significantly increased microglial LAG3 staining intensity. Moreover, in contrast with the effect of ECS, treatment with the LAG3 mAb also significantly elevated LAG3 expression (Fig. 5g).

To provide further evidence for the antidepressant effects of a chronic regimen of LAG3 mAb administration and compare these effects with those of the SSRI drug escitalopram (ESC, Cipralex®), we conducted an additional experiment. Following 5 weeks of CUS exposure and verification of anhedonia in the sucrose preference and reduction of social exploration, mice were chronically administered (i.p.) anti-LAG3 mAb or isotype IgG antibody (Fig. 5h). Injections were given every 4 days over a 3-week period, for a total of 6 injections. Each of these groups was divided into two subgroups, injected daily (i.p.) with either ESC (10 mg/kg) or saline. A group of non-stressed mice served as a control for the general effects of CUS.

Compared with pretreatment levels, sucrose preference was significantly elevated after treatment with the anti-LAG3 mAb, whereas treatment with the IgG antibody or treatment with ESC, either with IgG or LAG3 mAb, had no such effect (Fig. 5i). The levels of SE were significantly elevated after treatment with the anti-LAG3 mAb, as well as after ESC alone (i.e., with the IgG antibody). In contrast, treatment with ESC together with the anti-LAG3 mAb had no effect on SE (Fig. 5j). In the FST, there was a trend for CUS-induced increase in immobility and its reversal by LAG treatment, but this finding did not reach statistical significance (Fig. 5k). Analysis of the treatment effects on microglial morphology demonstrated that LAG mAb treatment reversed the CUS-induced decrease in total cell area in SAL- but not in ESC-injected mice (Fig. 5l). Processes number were reduced in both IgG- and LAG-treated SAL-injected mice (compared with no-stress controls) (Fig. 5m). Processes length was significantly reduced in CUS-exposed IgG-treated mice (compared with CON mice) and this reduction was completely rescued by the LAG3 mAb treatment in SAL-, but not ESC-injected mice (Fig. 5n). Finally, the CUS-induced decrease in the number of newborn (DCX-positive) neurons in the hippocampal DG was reversed by LAG3 mAb treatment (which induced even greater levels of neurogenesis than in controls) and to a lesser extent also by ESC. In contrast, the group treated with both LAG3 mAb and ESC displayed no such improvement (Fig. 5o), in accord with the negative interaction between the two drugs with respect to the behavioral and microglial effects.

To examine whether the effects of the LAG3 mAb could directly influence microglia by exerting microglial checkpoint inhibition, we pre-treated cultures of murine BV-2 microglia with the LAG3 mAb, followed by 24-h exposure to the immune stimulator Poly I:C. Exposure to Poly I:C at 1 µg/ml resulted in significantly elevated levels of the cytokine TNFα in the cell media ($F_{5,14} = 214.5$, $p < 0.001$). Preincubation of the cells with the LAG3 antibody, increased the levels of TNFα cytokine in a concentration-dependent manner, with 10 µg/ml remaining non-effective while 20 µg/ml ($p < 0.01$ versus Poly I:C group) up to 50 µg/ml ($p < 0.001$) gradually increasing the TNFα levels.

Given that the anti-LAG3 mAb was peripherally injected, we tested if the antibody enters the brain. To this end, we used brain tissue sections from mice that were either acutely (Fig. 5q) or chronically (Fig. 5r) injected (i.p.) with the anti-LAG3 mAb, co-stained with anti-rat Cy3-IgG for detection of the anti-LAG3 antibody together with anti-CD31 as a vascular marker. Anti-LAG3 positive staining was found in several brain regions, such as the sub-ventricular zone (SVZ), white matter tracks (e.g., corpus callosum), hippocampus and thalamus. In both the acute and chronic treatment conditions there was evidence for anti-LAG3 positive staining presence in the brain parenchyma, beyond the vascular staining. Such data indicate mobilization of the antibody from the periphery and into the CNS. In separate sections, we co-stained with anti-rat Cy3-IgG for detection of the anti-LAG3 antibody together with anti-IBA1 antibody. Anti-LAG3 staining was found in close proximity to microglia, in both the acute (Fig. 5s) or chronic (Fig. 5t) treatment conditions.

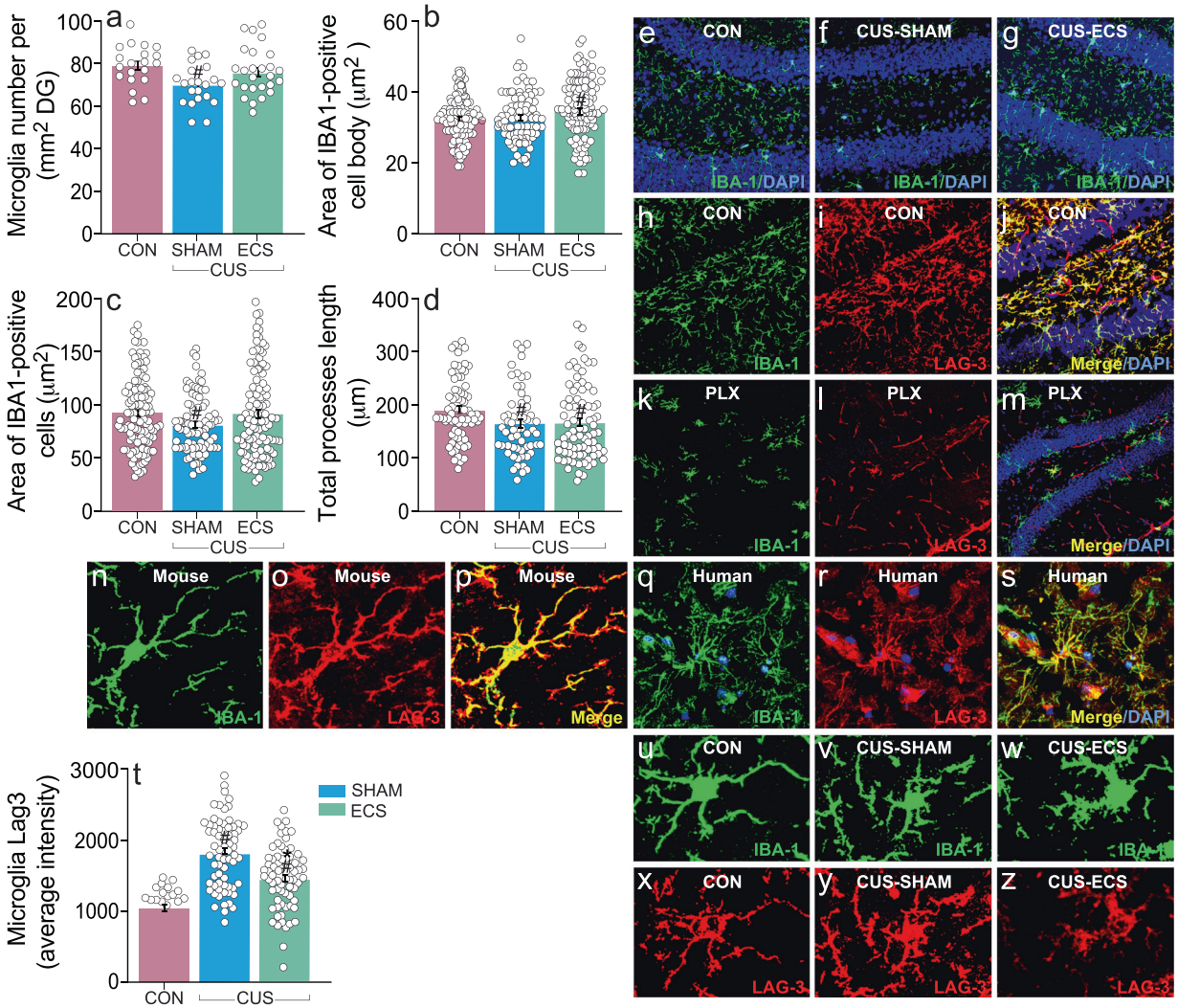

Fig. 4 Effects of ECS on microglia number, morphology and LAG-expression. a The CUS-induced reduction in DG microglia density exhibited by SHAM-treated mice, and its reversal in ECS-treated mice, were reflected by a significant overall group difference ($F_{2,\ 65} = 4.44$, $p < 0.02$; $p < 0.05^{\#}$ compared with the other two groups) ($n = 20$–26 DG images). Data for this and the other morphological analyses was obtained from $n = 5$–7 mice per condition. **b** CUS-exposed ECS-treated mice showed significantly enlarged IBA1-labeled cell bodies of DG microglia, reflected by a significant overall group difference ($F_{2,\ 308} = 3.29$, $p < 0.04$; $p < 0.02^{\#}$ compared with the other two groups; $n = 94$–109 DG microglia). **c** CUS-exposed, SHAM-treated mice exhibited a significant reduction in the area of IBA1-positive cells, which was reversed by ECS. This was reflected by a significant overall group difference ($F_{2,\ 305} = 3.2$, $p < 0.05$; $p < 0.03^{\#}$ compared with the CON group; $n = 90$–110 DG microglia). **d** CUS exposure produced an overall decrease in the length of microglial processes, reflected by a significant group difference ($F_{2,\ 211} = 3.45$, $p < 0.05$; $p < 0.03^{\#}$ compared with the CON group; $n = 60$–84 DG microglia). Representative fluorescent micrographs of IBA-1 labeled (green) hippocampal microglia from Control **e**, and CUS-exposed SHAM-treated **f** or ECS-treated **g** mice. Cell nuclei were also labeled (DAPI = blue). Representative fluorescent micrographs of the DG of a non-stress control mouse, labeled with either IBA-1 **h**, or LAG3 **i**) antibody, or double-labeled with the two antibodies **j**, demonstrate that all microglia (green) expressed LAG3 protein (red). LAG3 staining was also expressed by cells associated with blood vessels. Representative fluorescent micrographs of microglia remaining in the DG of a PLX-treated non-stressed mouse, labeled with either IBA-1 **k**, or LAG3 **l** antibody, or double-labeled with the two antibodies **m**, demonstrate the reduction of LAG3 staining in most microglia, with no apparent effect of PLX on LAG3 staining of blood vessel-associated cells. Immunohistochemical staining of a typical IBA-labeled microglia **n**, with LAG3 staining (red) of the membrane of both soma and processes **o**, as verified by double-labeling with the two antibodies **p**. Representative fluorescent micrographs of a microglia cell within the human prefrontal cortex, labeled with a P2Y12R antibody **q**, LAG3 antibody **r**, or both antibodies **s**. **t** CUS induced a significant increase in LAG3 levels (average intensity), reflected by an overall group difference ($F_{2,187} = 35.7$, $p < 0.001$; $p < 0.01^{\#}$ compared with the CON group; $p < 0.01^{*}$ compared with the SHAM treated group; $n = 30$–80 DG microglia, 5 brains/condition). Representative fluorescent micrographs of microglia cells from control **u** mice or CUS-exposed mice treated with SHAM **v** or ECS **w**. In the IBA-labeled microglia (green, top picture), LAG3 staining intensity (red, bottom picture) is greater in the microglia from a CUS-exposed SHAM-treated mouse than in microglia from a non-stress control (CON) mouse and a CUS-exposed ECS-treated mouse.

DISCUSSION

The findings of the present study show that depletion of most brain microglia did not trigger depressive-like symptoms or other emotional and cognitive alterations and did not prevent the development of depressive-like symptoms following exposure to CUS. These findings do not corroborate our previous proposal that normal functioning of microglia plays an important role in the maintenance of mood and emotional responsiveness, and that the

decline in microglia numbers and the morphological degeneration that are induced by exposure to CUS underlie the development of depression [21]. The simplest conclusion from the present findings is that in the adult brain, quiescent microglia under physiological conditions are not involved in regulation of mood and behavior and do not mediate the responsiveness to stressors. However, it is difficult to reconcile such a conclusion with a large body of evidence showing that microglia do play a role in neurobehavioral regulation and neurogenesis under quiescent conditions [40, 85–88], as well as in the development of stress-induced depression [21–23, 36–38, 52]. Thus, it is possible that during the microglia depletion process, the brain undergoes adaptive changes and other cells assume at least

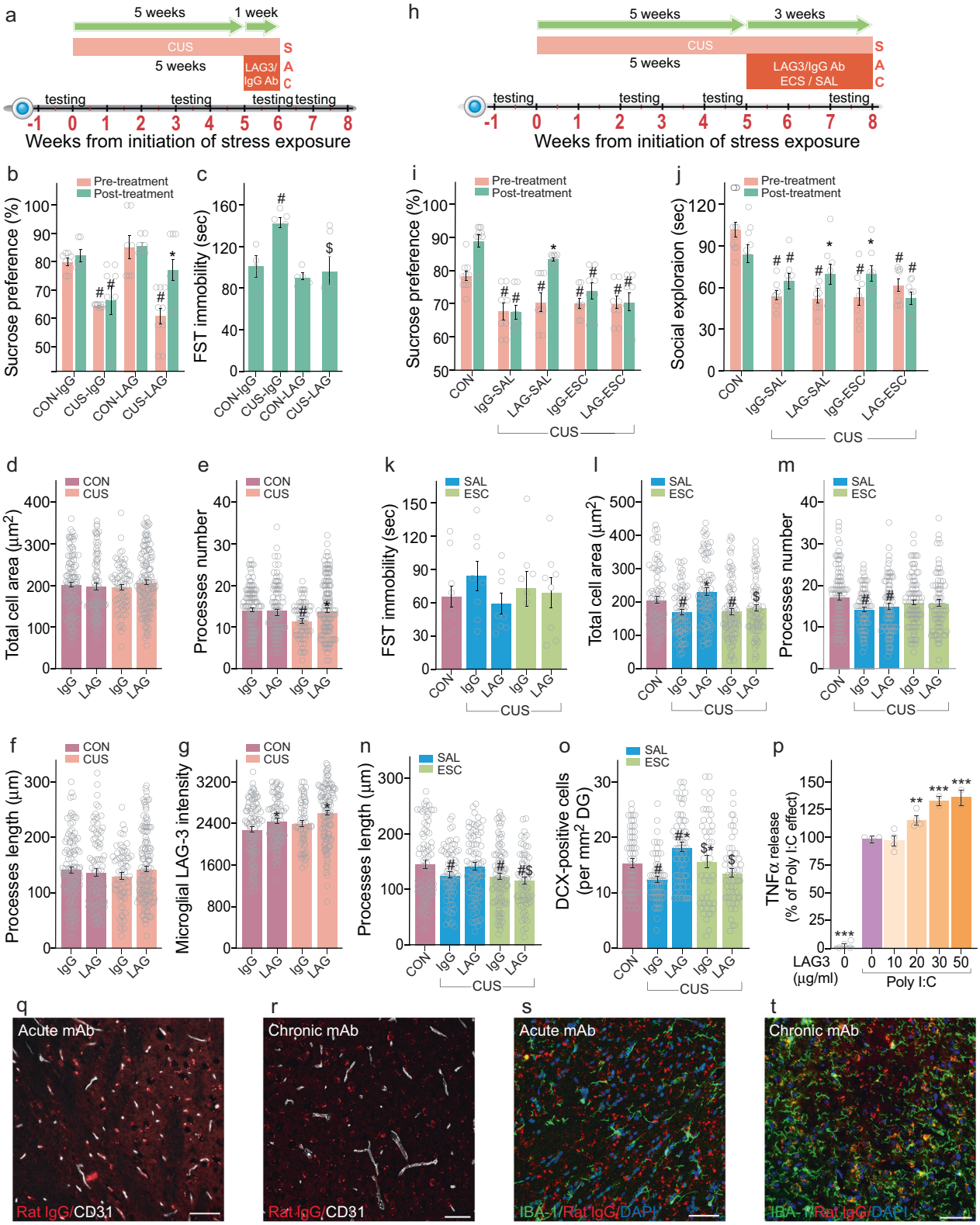

Fig. 5 Effects of acute and chronic administration of LAG3 mAb on depressive-like symptomatology, microglial morphology and neurogenesis in CUS-exposed mice. a Timeline of the acute experiment. **b** A significant three-way interaction was found among exposure (CUS/CON), treatment (IgG/LAG) and time (pre-/post-treatment) in the sucrose preference test ($F_{1,26} = 4.27$, $p < 0.05$; $p < 0.05^{\#}$ compared with their respective pre- and post-treatment CON groups; $p < 0.01^{*}$ compared with the respective pre-treatment test). **c** In the FST, there were significant effects of CUS exposure ($F_{1,18} = 4.66$, $p < 0.05$; $p < 0.05^{\#}$ compared with both CON groups) and drug treatment ($F_{1'18} = 5.79$, $p < 0.05$; $p < 0.05^{\$}$ compared with the CUS-IgG group). **d** Analysis of the total microglia cell area showed no significant differences among the groups. **e** Analysis of the number of processes revealed a significant CUS exposure by drug treatment interaction ($F_{1,429} = 4.26$, $p < 0.05$; $p < 0.05^{\#}$ compared with both CON groups; $p < 0.05^{*}$ compared with the CUS-IgG group). **f** The effects of exposure and treatment on processes' length were similar to those on the number of processes, but these findings did not reach statistical significance. **g** Analysis of the intensity of LAG staining within microglia revealed significant effects of both CUS exposure ($F_{1,\ 429} = 12.60$, $p < 0.0001$) and LAG treatment ($F_{1,\ 429} = 9.15$, $p < 0.01$; $p < 0.05^{\#}$ compared with the respective CON group). $n = 443$ cells from 22 mice. **h** Timeline of the chronic experiment. **i** Analysis of the sucrose preference results, using repeated-measures ANOVA, revealed a significant two-way (groups by time) interaction ($F_{1,37} = 3.454$, $p < 0.02$; $p < 0.05^{\#}$ compared with their pre- and post-treatment CON groups; $p < 0.05^{*}$ compared with its pre-treatment levels. **j** Analysis of the SE results, also revealed a significant group by time interaction ($F_{1,37} = 5.43$, $p < 0.01$; $p < 0.05^{\#}$ compared with their pre- and post-treatment CON groups ($p < 0.05^{\#}$) and $p < 0.05^{*}$ compared with their respective pre-treatment levels). **k** In the FST, there was a trend towards increased CUS-induced immobility and its reversal by the LAG treatment, but these findings did not reach statistical significance. **l** Analysis of the total microglia cell area showed a significant difference between the groups ($F_{4,398} = 7.51$, $p < 0.0001$; $p < 0.05^{\#}$ compared with the CON group; $p < 0.05^{*}$ compared with the SAL-IgG group; $p < 0.05^{\$}$ compared with the SAL-LAG group). **m** Processes number analysis revealed a significant difference between the groups ($F_{4,\ 397} = 2.51$, $p < 0.05$; $p < 0.05^{\#}$ compared with the CON group). **n** Processes length analysis also showed a significant difference between the groups ($F_{4,\ 397} = 3.84$, $p < 0.01$; ($p < 0.05^{\#}$ compared with the CON group; $p < 0.05^{\$}$ compared with the SAL-LAG group). $n = 403$ cells from 31 animals. **o** Newborn (DCX-positive) neurons density in the hippocampal dentate gyrus (DG) was significantly lower in CUS-exposed IgG-treated mice than in CON (f4,288 = 8.09, $p < 0.001$; $p < 0.05^{\#}$ compared with the CON group; $p < 0.05^{*}$ compared with the SAL-IgG group; $p < 0.05^{\$}$ compared with the SAL-LAG group). $n = 293$ slices from 31 mice. **p** Production of TNFα protein by BV-2 microglia cell cultures stimulated for 24 h by Poly I:C (1 μg/ml) and treated with increasing concentrations of LAG3 mAb (0–50 μg/ml). There was a significant differences between the groups ($F_{5,14} = 214.5$, $p < 0.001$), with Poly I:C producing a marked elevation in TNFα levels in the cell media, and the LAG3 mAb inducing a concentration-dependent augmentation of this effects ($p < 0.01^{**}$ compared with the Poly I:C only group); $p < 0.001^{***}$ compared with the Poly I:C only group). Representative images of co-staining with a vascular marker (CD31, white) together with anti-rat Cy3-IgG for detection of the anti-LAG3 antibody (red), in brain sections obtained from mice injected either acutely **q** or chronically **r**. Note anti-LAG3 mAb labeling in the brain parenchyma, beyond the vascular staining. (Representative images of co-staining with the microglia marker IBA-1 (green), together with anti-rat Cy3-IgG (red) and nuclear staining with DAPI (blue). Note the anti-LAG3 mAb labeling in close proximity to microglia, following both the acute **s** and chronic **t** treatments. Staining was conducted in $n = 3$ mice per group; scale bar = 50 μm.

some of the functions that are normally executed by microglia, including the promotion of CUS-induced depression (Fig. 6). This hypothesis is supported by the present finding that microglia depletion not only results in down-regulation of microglial genes but also induces an up-regulation of many genes, as well as down-regulation of non-microglial genes (https://www.ncbi.nlm.nih.gov/geo/query/acc.cgi?acc=GSE123027). Furthermore, previous research has demonstrated that microglia-depletion in PLX-treated mice induces various morphological and transcriptional changes in adult mature and newborn neurons [40, 89], astrocytes (which exhibit increased expression of various markers, including GFAP and S100B [90, 91] and are more reactive to environmental challenges [92]), and endothelial cells [91].

The present findings that ECS produced an increase in microglial soma area and overall size, along with reduced processes length and suppression of microglial LAG3 checkpoint expression, corroborate previous studies reporting that ECS induces microglia activation [61, 62]. The mechanism for this effect may involve stimulation of gamma oscillations, which are induced by ECS [93], and have recently been found to produce microglia proliferation, as well as morphological and molecular markers of microglial activation, including increases in soma size and an upregulation of hippocampal M-CSF and GM-CSF [94, 95]. Thus, the effects of ECS may be similar to those produced by exogenous administration of other microglia stimulators, such as M-CSF, GM-CSF, and LPS, in various models of depression in rodents [50–53, 96]. Together, these findings suggest that under conditions that involve microglia decline and degeneration, antidepressant procedures should harness microglia by stimulating these cells to their homeostatic activation levels, thereby allowing the microglia to normalize the neuro-behavioral abnormalities associated with these conditions (Fig. 6). Interestingly, in mouse models of neuroinflammation (experimental autoimmune encephalomyelitis and LPS administration), ECS was found to reduce the number of activated microglia and diminish the expression of activation markers [58, 59]. Together with the present findings, these results suggest that the effects of ECS depend on the inflammatory context of the individual and that microglia homeostasis can be restored by ECS under both hypo- and hyper-activation conditions.

Adult neurogenesis is considered an important mechanism of action of various antidepressants [42], including ECT [71]. Recent findings demonstrated several effects of microglia, in general [41], and DG microglia, in particular [97], on adult neurogenesis. Moreover, the interactions between microglia processes and the dendrites of adult newborn neurons play a cardinal role in synapse pruning, formation and maintenance, and integration of newborn neurons into functional brain circuitry [40]. The results of the present study extend these findings by showing that the neurogenesis-enhancing effects of ECS are based on the effects of this procedure on microglia. This is evidenced by the findings that ECS-induced neurogenesis enhancement as well as the expression of the neurogenesis-related gene *sox-11* were abrogated by microglia depletion as well as by minocycline. Interestingly, similar to our findings on microglia and depression, ablation of neurogenesis by various pharmacological or genetic methods usually does not result in depression and does not influence the development of CUS-induced depression. Still, the effects of monoaminergic antidepressants in chronically-stressed animals are completely blocked by neurogenesis ablation [43]. Thus, although it seems that microglia are not essential for the suppression of neurogenesis in depressed-like (CUS-exposed) mice, the microglia-mediated boosting of neurogenesis may be critical for mediating the anti-depressant effects of ECS.

Our results show that *Lag3* was the main transcript significantly and robustly reduced by ECS in both the RNA-Seq and validation analyses. The marked decrease in *Lag3* expression in PLX-treated, microglia-depleted mice, as well as the immunohistochemically verified expression of this molecule in all microglia cells, demonstrate its particular importance for microglia functioning. Our findings corroborate previous studies demonstrating the expression of *Lag3* in microglia isolated from the human or mouse

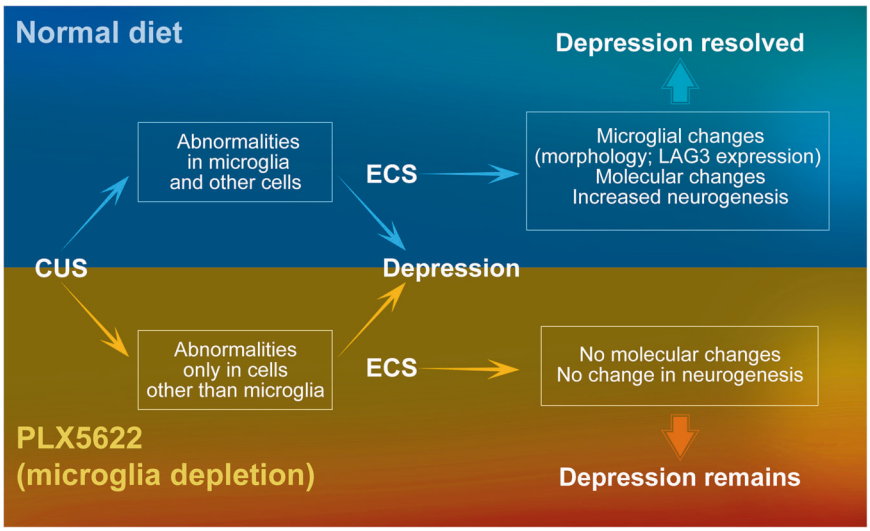

Fig. 6 A model depicting the role of microglia in the development of chronic unpredictable stress (CUS)-induced depression and its reversal by ECS. In control mice (receiving a normal diet), neurobehavioral functioning and CUS-induced depression are supported by microglia and by other brain cells. Under these conditions, ECS-induced activation of microglia via suppression of *Lag3* expression in these cells enhances hippocampal neurogenesis and alters the transcription by other cells of genes involved in immune regulation, neurogenesis, endocannabinoids and dopaminergic signaling. It is suggested that in microglia-depleted mice (treated with a PLX5622 diet) brain cells other than microglia undergo adaptive changes that can support normal neurobehavioral functioning and CUS-induced depression. However, without microglia (or when microglial activation is prevented by minocycline) ECS can no longer enhance neurogenesis or produce any transcriptional changes, resulting in abrogation of the antidepressant effects of this procedure. Thus, although microglia are not crucial for the development of stress-induced depression, the effects of ECS are causally dependent on the microglial alterations induced by this procedure. Based on this model, it is suggested that at least in some forms of depression, stimulation of microglia activation and restoration of their normal activation levels constitutes the mechanism of action of ECS; therefore, interventions aiming to mimic ECS's effects on microglia, such as by administration of LAG3 mAb or other microglia stimulators, can be promising antidepressant candidates.

brain [79–81]. Although cells associated with blood vessels (possibly endothelial cells) also express LAG3, its presence in these cells does not seem to play a cardinal role in the antidepressant effects of ECS, given that PLX5622, which abrogated the effects of ECS, had no effect on endothelial LAG3. Previous research suggested that *Lag3* is expressed by neurons and serves as the receptor for alpha-synuclein in this cell type [98]. However, we did not find neurons to express this receptor (data not shown). It is possible that LAG3 expression in neurons is induced only under specific conditions, such as following exposure to alpha-synuclein.

Previous studies established the role of LAG3 as a checkpoint of peripheral immune cells [99, 100] and demonstrated that during conditions in which the levels of this receptor and its main ligand (MHCII) are elevated (including chronic infections and cancer), LAG3-mediated negative regulation contributes to the exhaustion and suppression of immune cells [101]. A recent study also demonstrated that in neurodegenerative conditions associated with tauopathy, both in experimental transgenic mouse models and post-mortem brains from patients with Alzheimer's disease or progressive supranuclear palsy, an initial microglial activation is followed by induction of the checkpoint genes *lag3* and *pd-l1*, which (together with several other genes) mediate microglia suppression [102]. Our findings are the first to demonstrate that LAG3 expression can be significantly elevated following exposure to CUS, suggesting that chronic stress, similar to cancer or neurodegeneration, enhances immune/microglial checkpoint expression, resulting in decline and degeneration of these cells. Furthermore, in accordance with the experimental oncology literature, we also found that LAG3 checkpoint blockade can mimic at least some of the effects of ECS on microglia and promote morphological changes suggestive of elevated activation status.

The locus of action of the LAG3 mAb treatment described herein is not clear. Because the LAG3 mAb was injected i.p., its effects could have begun in the periphery, where it blocks the signaling of endogenous LAG3, which is known to serve as a checkpoint in peripheral monocytes by reducing the differentiation and functioning of these cells [103]. Such peripheral effects could be indirectly translated into effects on microglia and the resulting antidepressant effects; however, our results argue that at least some of the effects of the LAG3 mAb are produced by direct interaction with brain microglia. Although previous research using intact animals revealed that only a very small percentage (0.1–0.2%) of peripherally-injected antibodies penetrate the brain [104, 105], ample evidence demonstrates that in chronically-stressed mice [106, 107], and depressed subjects [108, 109], the integrity of the blood-brain-barrier is reduced in association with the disruption of tight junctions in brain blood vessels. This allows the passage of various molecules into the brain [107, 110]. In line with this, we show that in CUS-exposed mice, LAG3 mAb can be detected within the brain and can reach the vicinity of microglia. A possible disruption of the blood–brain barrier (BBB) integrity may also be associated with monocytes infiltrating the brain, which has previously been documented following exposure to chronic stress [111]. Upon brain infiltration peripheral monocytes begin to express high levels of Lag3 mRNA [112] and some of the effects of LAG3 blockade may thus be related to changes in infiltrating monocytes. Additional supportive evidence that LAG3 mAb can directly influence microglial functioning is derived from the finding that exposure of cultured microglia to this antibody augments Poly I:C-induced TNFα secretion. Considering that Poly I:C was previously shown to be the most potent inducer of MHC class II expression by cultured microglia [113] and that MHCII is the main ligand of the LAG3 receptors, which mediates checkpoint inhibition of target cells [82, 99, 100], this finding provides the first demonstration of the functionality of LAG3 as a microglial checkpoint that can mitigate microglia over-activation via an autocrine mechanism.

Translational research on the antidepressant properties of anti-LAG3 antibodies, suggests a novel therapeutic approach to treating of depression. Previous research has already

demonstrated that breaking microglial CX3CR1 checkpoint inhibition induces resilience to stress and prevention of depressive-like symptoms in mice [36–38]. The finding that LAG3 is directly involved in the therapeutic mechanism of action of ECS suggests that breaking microglial LAG3 checkpoint inhibition can also produce fast-acting and long-lasting antidepressant effects. Indeed, in our CUS model, the antidepressant effects of anti-LAG3 mAb in depressed-like mice were already evident 3 days after a single administration. Furthermore, a comparison of the effects of repeated injections of LAG3 vs. the SSRI escitalopram over a 3-week period showed complete reversal of depressive symptoms, as well as hippocampal neurogenesis, in anti-LAG3 mAb-treated mice, as compared with only partial reversal of the neurobehavioral symptomatology with escitalopram treatment. The latter finding is consistent with our previous report that chronic imipramine treatment was not effective in depressed-like mice with degenerated microglia [52].

Surprisingly, some of the therapeutic effects of the anti-LAG3 mAb treatment (on anhedonia, social withdrawal and neurogenesis) were abrogated by co-administration of escitalopram. This negative interaction may be related to the finding that escitalopram also blocked the modulatory effects of the anti-LAG3 mAb on microglial morphology. This finding suggests that in the current model, escitalopram produced microglia-suppressive effects that opposed the microglia-stimulating influence of the anti-LAG3 mAb. Such a conclusion is supported by previous research demonstrating that SSRIs often (but not always) decrease microglia activation [35, 114, 115] and that treatment of "depressed-like" (CUS-exposed) mice with an SSRI, while continuing the CUS exposure, decreased microglial reactivity [116]. The concurrent blockade of the microglial and antidepressant effects of LAG3 mAb by escitalopram further implicates microglia stimulation as the mechanism of action of the LAG3 mAb. Moreover, these findings suggest that LAG3 mAb treatment should serve as a replacement (rather than add-on) for SSRI therapy and may be particularly effective in depressed patients who are resistant (non-responsive) to SSRIs.

MATERIALS AND METHODS

Subjects

Subjects were 4 to 6 months old male WT C57BL/6 mice. Animals were housed in air-conditioned rooms (23 °C), with food and water ad libitum, and were kept in a reversed light/dark cycle, with lights off from 7:00 a.m. to 7:00 p.m. The numbers of mice per group in the behavioral, immunohistochemical and molecular experiments ($n = 6$–11, 4–7, and 3–6, respectively) were based on the minimal number of animals required to ensure sufficient statistical power, based on extensive previous experience in our laboratory and other laboratories conducting similar research. Subjects were randomly assigned to groups by allocating each consecutive cage (of 2–3 mice) on the animal rack (from top left to bottom right) to the next experimental group, repeating the process after reaching the last group in the experiment. All experiments were approved by the Hebrew University of Jerusalem Ethics Committee on Animal Care and Use.

Microglia manipulations with colony stimulating factor (CSF)-1 antagonist or minocycline administration. To induce microglia depletion, subjects were divided into two groups, treated with either a diet containing 1200 mg/g PLX5562 (Plexxicon Inc., U.S.A), a selective CSF-1 receptor kinase inhibitor, which when given chronically (i.e., for more than 2–3 weeks) induces near-complete microglial depletion [65, 90], or with a control diet (CDiet; containing identical ingredients but without PLX5562). Minocycline (Sigma, Israel) was administered via the drinking water at a dose of 40 mg/kg/day (this dose regimen has previously been found to be effective in counteracting chronic stress-induced microglial alterations and behavioral changes [52, 117]).

The chronic unpredictable stress (CUS) procedure

The CUS schedule comprised daily exposure to two stressors in a random order over a 5-week period. The list of stressors included cage shaking for 1 h with loud music and lights on; lights on during the entire night (12 h); lights-off for 3 h during the daylight phase; flashing (stroboscopic) light for 3 h; placement in a cold (4 °C) room for 1 h; mild restraint (in small ventilated cages) for 2 h, 45° cage tilt for 14 h; wet sawdust in the cage for 14 h; exposure to fox, ferret, bobcat, coyote or rat odor for 1 h; noise in the room for 3 h; and water deprivation for 12 h during the dark period.

The electroconvulsive stimulation (ECS) procedure

ECS was administered following CUS exposure and verification of the development of depressive-like symptoms. ECS was applied three times per week for 2.5 weeks for a total of eight sessions. Before each treatment, mice were lightly anesthetized with isoflurane and administered a single shock via ear clip electrodes, using a Ugo Basile ECS Unit (Varese, Italy). The following shock parameters were used: frequency = 100 pulses per sec, current = 18 mA, shock duration = 0.3 s, and pulse width = 0.5 ms. To control for the effects of ECS, half the mice in each experiment underwent SHAM treatment, in which they were exposed to the same procedure but no current was applied through the electrodes.

Anti-LAG3 and escitalopram treatments

Anti-LAG3 (Anti-mouse BLG-125204) or IgG (Anti-mouse IgG1, BLG-400414) antibody (100 µg/mouse; Biolegend, CA, USA) was injected i.p. in a volume of 10 ml/kg saline. In one experiment, the antibodies were injected once (following verification of the development of CUS-induced depression). Sucrose preference and despair in the forced swim test (FST, see below) were assessed 3 and 5 days, respectively, after treatment. In another experiment, antibodies were injected every 4 days for a total of six injections, over a 3-week period. Escitalopram (Teva, Israel) or saline was injected daily over 3 weeks. The escitalopram dose was 5 mg/kg during the first week and 10 mg/kg in the next two weeks. Mice were sacrificed 4–5 days following the last injection.

Behavioral measurements

Social exploration. Each subject was placed in an observation cage and allowed to habituate to the cage for 15 min, following which a male juvenile was placed in the cage. Social exploration (SE), defined as the time of near contact between the nose of the subject and the juvenile conspecific, was then recorded for 2 min, using computerized in-house software. During this test, and all other behavioral tests, the investigators were blinded to the group allocation.

The elevated plus maze test. In this test, an elevated plus-shaped apparatus was used, which has two open and two enclosed arms. In the beginning of the test, each mouse was placed in the middle of the arena. The distance traveled and the time spent in the open arm was measured over a 3-min period. Behavior was analyzed automatically using the EthoVision XT video tracking system and software (Noldus, the Netherlands).

The spatial object recognition test. Mice were habituated to a semi-circular test cage for three consecutive days. On the fourth day, mice were allowed to explore two identical objects until they reached a criterion (a total of 20 s of nose-directed exploration of the objects) or for 3 min. Mice who failed to explore the objects for at least 10 s were discarded from the experiment. Twenty-four hours later, mice were allowed to explore the two identical objects but this time, one of the objects was moved to a new location. Nose-directed exploration time for each of the two objects was recorded until the criterion was reached or for 3 min total.

Sucrose preference test. Following baseline adaptation to sucrose for 3–4 days, mice were presented, in the beginning of the dark phase of the circadian cycle, with two graduated drinking tubes, one containing tap water and the other a 1% sucrose solution for 4 h. Sucrose preference was calculated as the percentage of sucrose consumption out of the total drinking volume.

The Porsolt forced swim test. Mice were placed in a plexiglass cylinder (with a height of 30 cm and diameter of 20 cm) filled with 25 °C water. The time spent immobile, defined as the absence of all movement except for motions required to maintain the head above water, was recorded for six min, and automatically analyzed off-line using the EthoVision software (Noldus).

Immunohistochemistry

Animals were perfused transcardially with cold phosphate-buffered saline (PBS) followed by 4% paraformaldehyde in 0.1 M PBS, and the brains were quickly removed and placed in 4% paraformaldehyde. After 24 h, the brains were placed in 30% sucrose solution in PBS for 48 h and then frozen in optimal cutting temperature (OCT) compound. Coronal sections (8 µm, 14 µm, or 50 µm) were serially cut along the rostro-caudal axis of the dorsal hippocampus, using a cryostat (Leica, Wetzlar, Germany), and mounted on slides.

Microglia were visualized using a primary antibody of the microglial marker ionized calcium-binding adapter molecule-1 (IBA1; rabbit anti Iba-1 1:250, Wako, Japan), followed by a secondary antibody (goat anti rabbit, 1:200; Invitrogen, Carlsbad, CA, USA), as previously described [52]. The rate of neurogenesis in the hippocampus was measured by staining for doublecortin (DCX), using guinea pig anti-DCX (1:1000, Millipore, Chemicon, Tamecula, CA, USA) as the primary antibody, and biotin-SP-conjugated donkey anti-guinea pig (1:200; Jackson Laboratories, West Grove, PA, USA) as the secondary antibody, with final visualization using a conjugated streptavidin Ab (Jackson Laboratories, West grove, PA, USA), as previously described. Rabbit-anti P2RY12 1:250 was also used to visualize microglia (AnaSpec, Fremont, CA, USA), followed by a secondary antibody (goat anti-rabbit, 1:200; Invitrogen, Carlsbad, CA, USA). Microglial LAG3 was visualized using the monoclonal LAG3 MABF954 clone 4–10-C9 antibody (1:200, Millipore, MA, USA).

Image analysis

To assess the number of microglia (IBA1-positive cells) and DCX-positive neurogenic cells in the hippocampus, we captured images using a Nikon Eclipse microscope and camera. Cells were manually counted using 10X magnification in a defined area exclusively containing the dentate gyrus (DG) region of the dorsal hippocampus for each slide, using Nikon Imaging Elements Software or ImageJ/FIJI software. Four sections of each brain were counted. Confocal images were captured using an Olympus FV-1000 confocal microscope. Slices were imaged at 0.165–0.2 µm/pixel in the XY dimension and at 0.5 µm steps in the *Z* dimension (unless otherwise stated in the figure legend), using collapsed z-stacks. Microglia cell processes length was measured by capturing images at ×40 magnification and by manual tracing of the processes of all IBA1-positive cells in these sections throughout the Z-stacks, using the ImageJ/FIJI software. Cells displaying more than two standard deviations (SDs) in one of the two measures (cell body area or cell size area) were omitted from the calculations. The investigators were blinded to the group allocation during all stages of the immunohistochemical analyses.

Real-time quantitative polymerase chain reaction (PCR) analysis

Mice were sacrificed by decapitation. Each brain was quickly removed, placed on an ice-cold glass plate, and the hippocampus was dissected out under a binocular. Tissues were weighed, flash frozen in liquid nitrogen and stored at −80 °C until RNA extraction. RNA was extracted using PerfectPure RNA extraction kit (5 PRIME, Darmstadt, Germany). RNA samples (2 µg) were reverse transcribed using the QuantiTect Reverse Transcription Kit from Qiagen (Hilden, Germany), including DNase treatment of contaminating genomic DNA. Expression of mRNA was determined by qPCR, using glyceraldehyde-3-phosphate dehydrogenase (*Gapdh*) as a normalizing gene, as previously described [118]. We designed primers using PrimerQuest IDT (Integrated DNA Technologies, Inc, San Diego, CA, USA). The following primers were used. *Gapdh*, Forward: TCT CCC TCA CAA TTT CC; Reverse: GGG TGC AGC GAA CTT TA. *Drd1*, Forward: CTT CTG GAA GAT GGC TCC TAA C; Reverse: CCC TAA GAG AGT GGA CAG GAT A. *Tdo2*, Forward: CAT CGT GTG GTG GTC ATC TT; Reverse: CTG ATG CTG GAG ACA GGT ATT C. *Iba1*, Forward: GAC GTT CAG CTA CTC TGA CTT T; Reverse: GTT GGC CTC TTG TGT TCT TTG. *Lag3*, Forward: TCA TCA CAG TGA CTC CCA AAT C; Reverse: GCC ACA CAA ATC TTT CCT TTC C. *Cd180*, Forward: CTC CGA AAC CTG TCT CAC TTA C; Reverse: GTT CTA GCT GAG GGC ATT CTT. *Sox11*, Forward: CTC CAT CAC TCG GCT TTC TTA T; Reverse: CTC TCT TCC AAG TGT CCA CAA A. *Plag24e*, Forward: CAG GAA CCC ATA CTG TGA AGA; Reverse: GCT GGT AGG AGA GTG TGA TAA AT, *P2ry12* Forward: CCT TAA CAC TAG AGG CAG CAA; Reverse: CAT TCA AGC AGC AGG CAT TT.

Normal and mock reversed transcribed samples (in the absence of reverse transcriptase) and no template controls (total mix without cDNA) were run for each of the examined mRNAs. qPCR reactions were subjected to an initial step of 15 min at 95 °C to activate the HotStar Taq DNA polymerase, followed by 40 cycles consisting of 15 s at 94 °C, 30 s at 60 °C and 30 s at 72 °C. Fluorescence was measured at the end of each elongation step. Data were collected and analyzed using the StepOnePlus instrument and software (Thermo Fisher Scientific) and a threshold cycle value Ct was calculated from the exponential phase of each PCR sample. Expression levels of mRNAs were calculated and expressed in relative units of SYBR Green fluorescence.

RNA sequencing

PolyA-based mRNA was selected using oligodT beads, followed by fragmentation, and first-strand and second-strand synthesis reactions. Illumina libraries were constructed while performing the end repair, A base addition, adapter ligation, and PCR amplification steps with SPRI beads cleanup in-between steps. Indexed samples were pooled and sequenced in an Illumina HiSeq 2500 machine in a single read mode.

Bioinformatics analysis

Adapters were trimmed using the cutadapt tool. Following adapter removal, reads that were shorter than 40 nucleotides were discarded (cutadapt option –m 40). Reads that had either a percentage of Adenine bases above 50% or a percentage of Thymine bases above 50% were discarded using a custom script. TopHat (v2.0.10) was used to align the reads to the mouse genome (mm10). Counting reads on mm10 RefSeq genes (downloaded from igenomes) was completed with HTSeq-count (version 0.6.1p1). Differential expression analysis was performed using DESeq2 (1.6.3). Raw p values were adjusted for multiple testing (*q* value, false discovery rate) using Benjamini and Hochberg's procedure. All of the RNA-Seq data reported herein have been deposited in NCBI's Gene Expression Omnibus and are accessible through GEO Series accession number GSE123027.

In vitro experiment in Poly I:C activated BV-2 cells

Murine BV-2 microglia cells were cultured at 37 °C in a humidified atmosphere with 5% CO2 in high D-glucose (4.5 g/L) Dulbecco's modified Eagle's medium (Sigma, Rehovot, Israel) supplemented with 5% heat-inactivated fetal bovine serum, streptomycin (100 µg/ml), and penicillin (100 units/ml) and sodium pyruvate (1 mM; all from Biological Industries Ltd., Kibbutz Beit Haemek, Israel). 24 h before the experiments with Poly I:C stimulation, the BV-2 cells were split into 24 well plates, 2×10^5 cells per well, covered with 1 ml of growth medium and allowed to attach overnight.

Poly I:C (Sigma, P1530) was first dissolved in sterile, molecular-grade water to the concentration of 10 mg/ml (following the manufacturer's instructions). The stock solution was further diluted to a concentration of 1 mg/ml in sterile PBS, and the aliquots stored at −20 °C. The final concentration of Poly I:C in the cell medium used to activate the BV-2 cells was 1 µg/ml, which was chosen based on pilot concentration- and time-dependent experiments where the levels of TNFα released in response to Poly I:C were estimated using enzyme-linked immunosorbent assay (ELISA) on cell-conditioned and cell free media.

The BV2 cells were activated with 1 µg/ml of Poly I:C for 24 h. The anti-mouse LAG3 antibody (BioXCell, clone C9B7W, BE0174) was introduced 1 h before Poly I:C activation, in concentrations of 10 or 20 or 30 or 50 µg/ml. After 24 h of Poly I:C activation, the media along with the cells were collected, spun down for 5 min at 2000 rpm and the supernatants (without the cell pellets) were frozen at −80 °C till further analysis. The concentrations of TNFα were determined using mouse TNFα ELISAs following the protocol recommended by the supplier (R&D Systems, Minneapolis, MN, USA). The serum in the culture media did not interfere with the assays. The ELISA measurements were carried out using a Tecan Sunrise absorbance plate reader with 450 nm filter (and 620 nm filter background correction) and the data (OD values) were processed using Magellan TM and MS Excel software. The raw OD values obtained using absorbance microplate reader were transformed to relative % values, with the OD value obtained for Poly I:C assigned as 100% activation (maximal inflammatory response).

Assessment of anti-LAG3 mAb brain penetration

Brains from mice that were acutely or chronically (every 4 days, over a 3-week period, for a total of 6 injections) injected (i.p.) with an anti-LAG3 mAb were dissected and fixed 5 days after the last injection. 8-micron thick cryo-sections were washed with PBS for 15 min at RT and then incubated for 1 h at RT with blocking solution (10% BSA, 10% normal horse serum,

0.05% triton X-100 in PBS). Slides were incubated with primary antibodies (diluted in 2.5% BSA, 2.5% normal horse serum, 0.05% triton X-100 in PBS) at 4 °C overnight. Slides were then washed with PBS, incubated with secondary antibodies for 1 h at RT, washed, and mounted with DAPI Fluoromount-G.

The primary antibodies used were: hamster anti-mouse CD31 (1:100, Bio-Rad cat No. MCA1370Z) and rabbit anti IBA-1 (1:200, FUJIFILM Wako Pure Chemical Corporation, cat No. 019-19741). For detecting anti-LAG3 antibodies, Cy3 donkey anti-rat IgG (1:500, Jackson cat No.712165153) was used as a primary antibody. The secondary antibodies used were: Alexa Fluor 647 goat anti-Armenian hamster (1:500, Jackson cat No.127605160) and Alexa Fluor 488 donkey anti-rabbit IgG (1:200, Jackson cat No.711545152).

Images were taken using a Nikon eclipse Ni confocal microscope, with either 20 or 40 lenses, with 1 µm intervals. Maximal projection images of 8-micron thick sections are presented.

Statistical analysis

All data are presented as mean ± SEM. Statistical comparisons were computed using SPSS version 26.0 software and consisted of *t* tests and one-way or two-way analysis of variances (ANOVAs) (using Wilks' Lambda), followed by post hoc analyses using the Fisher's least significant difference or Bonferroni-corrected *t* tests, when appropriate. There were no significant differences in the variance between the groups that were statistically compared. In the in vitro experiments, the effects of various concentrations of the anti-mouse LAG3 antibody were compared to the PBS (vs. Vehicle) + Poly I:C group and expressed as % values as well. The statistical analysis was performed on % values; $n = 2–4$ experiments, in which all the treatments were tested in duplicates in each experiment. The Graph Pad Prism software v9.0.2. (San Diego, CA, USA) was used for statistical analysis. The data are expressed as the mean ± S.E.M. and analyzed for statistical significance using one-way ANOVA, followed by Dunnett's post-hoc tests for comparisons to the PBS + Poly I:C group. $p < 0.05$ was considered significant.

DATA AND MATERIALS AVAILABILITY

The RNA-Seq data discussed in this publication have been deposited in NCBI's Gene Expression Omnibus and are accessible through GEO Series accession number GSE123027.

REFERENCES

1. Krishnan V, Nestler EJ. Linking molecules to mood: new insight into the biology of depression. Am J Psychiatry. 2010;167:1305–20.
2. Duman RS, Voleti B. Signaling pathways underlying the pathophysiology and treatment of depression: novel mechanisms for rapid-acting agents. Trends Neurosci. 2012;35:47–56.
3. Enache D, Pariante CM, Mondelli V. Markers of central inflammation in major depressive disorder: a systematic review and meta-analysis of studies examining cerebrospinal fluid, positron emission tomography and post-mortem brain tissue. Brain Behav Immun. 2019;72:268–75.
4. Yirmiya R, Weidenfeld J, Pollak Y, Morag M, Morag A, Avitsur R, et al. Cytokines, "depression due to a general medical condition," and antidepressant drugs. Adv Exp Med Biol. 1999;461:283–316.
5. Maes M, Yirmyia R, Noraberg J, Brene S, Hibbeln J, Perini G, et al. The inflammatory & neurodegenerative (I&ND) hypothesis of depression: leads for future research and new drug developments in depression. Metab Brain Dis. 2009;24:27–53.
6. Raison CL, Capuron L, Miller AH. Cytokines sing the blues: inflammation and the pathogenesis of depression. Trends Immunol. 2006;27:24–31.
7. Dantzer R, O'Connor JC, Freund GG, Johnson RW, Kelley KW. From inflammation to sickness and depression: when the immune system subjugates the brain. Nat Rev Neurosci. 2008;9:46–56.
8. Miller AH, Raison CL. The role of inflammation in depression: from evolutionary imperative to modern treatment target. Nat Rev Immunol. 2016;16:22–34.
9. Howren MB, Lamkin DM, Suls J. Associations of depression with C-reactive protein, IL-1, and IL-6: a meta-analysis. Psychosom Med. 2009;71:171–86.
10. Dowlati Y, Herrmann N, Swardfager W, Liu H, Sham L, Reim EK, et al. A meta-analysis of cytokines in major depression. Biol Psychiatry. 2010;67:446–57.
11. Kern S, Skoog I, Börjesson-Hanson A, Blennow K, Zetterberg H, Ostling S, et al. Lower CSF interleukin-6 predicts future depression in a population-based sample of older women followed for 17 years. Brain Behav Immun. 2013;32:153–8.
12. Hannestad J, DellaGioia N, Bloch M. The effect of antidepressant medication treatment on serum levels of inflammatory cytokines: a meta-analysis. Neuropsychopharmacology. 2011;36:2452–9.
13. Warner-Schmidt JL, Vanover KE, Chen EY, Marshall JJ, Greengard P. Antidepressant effects of selective serotonin reuptake inhibitors (SSRIs) are attenuated by antiinflammatory drugs in mice and humans. Proc Natl Acad Sci USA. 2011;108:9262–7.
14. Chung HS, Kim H, Bae H. Phenelzine (monoamine oxidase inhibitor) increases production of nitric oxide and proinflammatory cytokines via the NF-kappaB pathway in lipopolysaccharide-activated microglia cells. Neurochem Res. 2012;37:2117–24.
15. Nettis MA, Lombardo G, Hastings C, Zajkowska Z, Mariani N, Nikkheslat N, et al. Augmentation therapy with minocycline in treatment-resistant depression patients with low-grade peripheral inflammation: results from a double-blind randomised clinical trial. Neuropsychopharmacology. 2021;46:939–48.
16. Attwells S, Setiawan E, Rusjan PM, Xu C, Hutton C, Rafiei D, et al. Translocator protein distribution volume predicts reduction of symptoms during open-label trial of celecoxib in major depressive disorder. Biol Psychiatry. 2020;88:649–56.
17. Savitz JB, Teague TK, Misaki M, Macaluso M, Wurfel BE, Meyer M, et al. Treatment of bipolar depression with minocycline and/or aspirin: an adaptive, 2x2 double-blind, randomized, placebo-controlled, phase IIA clinical trial. Transl Psychiatry. 2018;8:27.
18. Raison CL, Rutherford RE, Woolwine BJ, Shuo C, Schettler P, Drake DF, et al. A randomized controlled trial of the tumor necrosis factor antagonist infliximab for treatment-resistant depression: the role of baseline inflammatory biomarkers. JAMA Psychiatry. 2013;70:31–41.
19. Rapaport MH, Nierenberg AA, Schettler PJ, Kinkead B, Cardoos A, Walker R, et al. Inflammation as a predictive biomarker for response to omega-3 fatty acids in major depressive disorder: a proof-of-concept study. Mol Psychiatry. 2016;21:71–79.
20. Arteaga-Henriquez G, Simon MS, Burger B, Weidinger E, Wijkhuijs A, Arolt V, et al. Low-grade inflammation as a predictor of antidepressant and anti-inflammatory therapy response in mdd patients: a systematic review of the literature in combination with an analysis of experimental data collected in the EU-MOODINFLAME Consortium. Front Psychiatry. 2019;10:458.
21. Yirmiya R, Rimmerman N, Reshef R. Depression as a microglial disease. Trends Neurosci. 2015;38:637–58.
22. Singhal G, Baune BT. Microglia: an interface between the loss of neuroplasticity and depression. Front Cell Neurosci. 2017;11:270.
23. Wohleb ES, Franklin T, Iwata M, Duman RS. Integrating neuroimmune systems in the neurobiology of depression. Nat Rev Neurosci. 2016;17:497–511.
24. Clark SM, Pocivavsek A, Nicholson JD, Notarangelo FM, Langenberg P, McMahon RP, et al. Reduced kynurenine pathway metabolism and cytokine expression in the prefrontal cortex of depressed individuals. J Psychiatry Neurosci. 2016;41:386–94.
25. Torres-Platas SG, Cruceanu C, Chen GG, Turecki G, Mechawar N. Evidence for increased microglial priming and macrophage recruitment in the dorsal anterior cingulate white matter of depressed suicides. Brain Behav Immun. 2014;42:50–59.
26. Bayer TA, Buslei R, Havas L, Falkai P. Evidence for activation of microglia in patients with psychiatric illnesses. Neurosci Lett. 1999;271:126–8.
27. Steiner J, Bielau H, Brisch R, Danos P, Ullrich O, Mawrin C, et al. Immunological aspects in the neurobiology of suicide: elevated microglial density in schizophrenia and depression is associated with suicide. J Psychiatr Res. 2008;42:151–7.
28. Li H, Sagar AP, Keri S. Microglial markers in the frontal cortex are related to cognitive dysfunctions in major depressive disorder. J Affect Disord. 2018;241:305–10.
29. Holmes SE, Hinz R, Conen S, Gregory CJ, Matthews JC, Anton-Rodriguez JM, et al. Elevated translocator protein in anterior cingulate in major depression and a role for inflammation in suicidal thinking: a positron emission tomography study. Biol Psychiatry. 2018;83:61–9.
30. Setiawan E, Wilson AA, Mizrahi R, Rusjan PM, Miler L, Rajkowska G, et al. Role of translocator protein density, a marker of neuroinflammation, in the brain during major depressive episodes. JAMA Psychiatry. 2015;72:268–75.
31. Hannestad J, DellaGioia N, Gallezot JD, Lim K, Nabulsi N, Esterlis I, et al. The neuroinflammation marker translocator protein is not elevated in individuals with mild-to-moderate depression: a [(1)(1)C]PBR28 PET study. Brain Behav Immun. 2013;33:131–8.
32. Bufalino C, Hepgul N, Aguglia E, Pariante CM. The role of immune genes in the association between depression and inflammation: a review of recent clinical studies. Brain Behav Immun. 2013;31:31–47.
33. Pantazatos SP, Huang YY, Rosoklija GB, Dwork AJ, Arango V, Mann JJ. Whole-transcriptome brain expression and exon-usage profiling in major depression

and suicide: evidence for altered glial, endothelial and ATPase activity. Mol Psychiatry. 2017;22:760–73.
34. Mahajan GJ, Vallender EJ, Garrett MR, Challagundla L, Overholser JC, Jurjus G, et al. Altered neuro-inflammatory gene expression in hippocampus in major depressive disorder. Prog Neuropsychopharmacol Biol Psychiatry. 2018;82:177–86.
35. Tynan RJ, Weidenhofer J, Hinwood M, Cairns MJ, Day TA, Walker FR. A comparative examination of the anti-inflammatory effects of SSRI and SNRI antidepressants on LPS stimulated microglia. Brain Behav Immun. 2012;26:469–79.
36. Hellwig S, Brioschi S, Dieni S, Frings L, Masuch A, Blank T, et al. Altered microglia morphology and higher resilience to stress-induced depression-like behavior in CX3CR1-deficient mice. Brain Behav Immun. 2016;55:126–37.
37. Rimmerman N, Schottlender N, Reshef R, Dan-Goor N, Yirmiya R. The hippocampal transcriptomic signature of stress resilience in mice with microglial fractalkine receptor (CX3CR1) deficiency. Brain Behav Immun. 2017;61:184–96.
38. Milior G, Lecours C, Samson L, Bisht K, Poggini S, Pagani F, et al. Fractalkine receptor deficiency impairs microglial and neuronal responsiveness to chronic stress. Brain Behav Immun. 2015;55:114–25.
39. Ekdahl CT, Kokaia Z, Lindvall O. Brain inflammation and adult neurogenesis: the dual role of microglia. Neuroscience. 2009;158:1021–9.
40. Reshef R, Kudryavitskaya E, Shani-Narkiss H, Isaacson B, Rimmerman N, Mizrahi A, et al. The role of microglia and their CX3CR1 signaling in adult neurogenesis in the olfactory bulb. Elife. 2017;6:e30809.
41. Sierra A, Beccari S, Diaz-Aparicio I, Encinas JM, Comeau S, Tremblay ME. Surveillance, phagocytosis, and inflammation: how never-resting microglia influence adult hippocampal neurogenesis. Neural Plast. 2014;2014:610343.
42. Miller BR, Hen R. The current state of the neurogenic theory of depression and anxiety. Curr Opin Neurobiol. 2015;30:51–58.
43. Surget A, Tanti A, Leonardo ED, Laugeray A, Rainer Q, Touma C, et al. Antidepressants recruit new neurons to improve stress response regulation. Mol Psychiatry. 2011;16:1177–88.
44. Du Preez A, Eum J, Eiben I, Eiben P, Zunszain PA, Pariante CM, et al. Do different types of stress differentially alter behavioural and neurobiological outcomes associated with depression in rodent models? A systematic review. Front Neuroendocrinol. 2021;61:100896.
45. Wohleb ES, Terwilliger R, Duman CH, Duman RS. Stress-induced neuronal colony stimulating factor 1 provokes microglia-mediated neuronal remodeling and depressive-like behavior. Biol Psychiatry. 2018;83:38–49.
46. Wohleb ES, Hanke ML, Corona AW, Powell ND, Stiner LM, Bailey MT, et al. β-Adrenergic receptor antagonism prevents anxiety-like behavior and microglial reactivity induced by repeated social defeat. J Neurosci. 2011;31:6277–88.
47. Hinwood M, Morandini J, Day TA, Walker FR. Evidence that microglia mediate the neurobiological effects of chronic psychological stress on the medial prefrontal cortex. Cereb Cortex. 2012;22:1442–54.
48. Frank MG, Baratta MV, Sprunger DB, Watkins LR, Maier SF. Microglia serve as a neuroimmune substrate for stress-induced potentiation of CNS pro-inflammatory cytokine responses. Brain Behav Immun. 2007;21:47–59.
49. Wang YL, Han QQ, Gong WQ, Pan DH, Wang LZ, Hu W, et al. Microglial activation mediates chronic mild stress-induced depressive- and anxiety-like behavior in adult rats. J Neuroinflammation. 2018;15:21.
50. Tong L, Gong Y, Wang P, Hu W, Wang J, Chen Z, et al. microglia loss contributes to the development of major depression induced by different types of chronic stresses. Neurochem Res. 2017;42:2698–711.
51. Cai Z, Ye T, Xu X, Gao M, Zhang Y, Wang D, et al. Antidepressive properties of microglial stimulation in a mouse model of depression induced by chronic unpredictable stress. Prog Neuropsychopharmacol Biol Psychiatry. 2020;101:109931.
52. Kreisel T, Frank MG, Licht T, Reshef R, Ben-Menachem-Zidon O, Baratta MV, et al. Dynamic microglial alterations underlie stress-induced depressive-like behavior and suppressed neurogenesis. Mol Psychiatry. 2014;19:699–709.
53. Gong Y, Tong L, Yang R, Hu W, Xu X, Wang W, et al. Dynamic changes in hippocampal microglia contribute to depressive-like behavior induced by early social isolation. Neuropharmacology. 2018;135:223–33.
54. Maes M, Song C, Yirmiya R. Targeting IL-1 in depression. Expert Opin Thera Targets. 2012;16:1097–112.
55. Goshen I, Kreisel T, Ben-Menachem-Zidon O, Licht T, Weidenfeld J, Ben-Hur T, et al. Brain interleukin-1 mediates chronic stress-induced depression in mice via adrenocortical activation and hippocampal neurogenesis suppression. Mol Psychiatry. 2008;13:717–28.
56. Bassett B, Subramaniyam S, Fan Y, Varney S, Pan H, Carneiro AMD, et al. Minocycline alleviates depression-like symptoms by rescuing decrease in neurogenesis in dorsal hippocampus via blocking microglia activation/phagocytosis. Brain Behav Immun. 2021;91:519–30.
57. Lisanby SH. Electroconvulsive therapy for depression. N Engl J Med. 2007;357:1939–45.
58. Goldfarb S, Fainstein N, Ben-Hur T. Electroconvulsive stimulation attenuates chronic neuroinflammation. JCI Insight. 2020;5:e137028.
59. Goldfarb S, Fainstein N, Ganz T, Vershkov D, Lachish M, Ben-Hur T. Electric neurostimulation regulates microglial activation via retinoic acid receptor alpha signaling. *Brain Behav Immun.* 2021;96:40–53.
60. Sepulveda-Rodriguez A, Li P, Khan T, Ma JD, Carlone CA, Bozzelli PL, et al. Electroconvulsive shock enhances responsive motility and purinergic currents in microglia in the mouse hippocampus. eNeuro. 2019;6:ENEURO.0056-19.2019.
61. Jinno S, Kosaka T. Reduction of Iba1-expressing microglial process density in the hippocampus following electroconvulsive shock. Exp Neurol. 2008;212:440–7.
62. van Buel EM, Sigrist H, Seifritz E, Fikse L, Bosker FJ, Schoevers RA, et al. Mouse repeated electroconvulsive seizure (ECS) does not reverse social stress effects but does induce behavioral and hippocampal changes relevant to electroconvulsive therapy (ECT) side-effects in the treatment of depression. PLoS One. 2017;12:e0184603.
63. Prinz M, Priller J. Microglia and brain macrophages in the molecular age: from origin to neuropsychiatric disease. Nat Rev Neurosci. 2014;15:300–12.
64. Mondelli V, Vernon AC, Turkheimer F, Dazzan P, Pariante CM. Brain microglia in psychiatric disorders. Lancet Psychiatry. 2017;4:563–72.
65. Dagher NN, Najafi AR, Kayala KM, Elmore MR, White TE, Medeiros R, et al. Colony-stimulating factor 1 receptor inhibition prevents microglial plaque association and improves cognition in 3xTg-AD mice. J Neuroinflammation. 2015;12:139.
66. Jansson L, Wennstrom M, Johanson A, Tingstrom A. Glial cell activation in response to electroconvulsive seizures. Prog Neuropsychopharmacol Biol Psychiatry. 2009;33:1119–28.
67. Tikka T, Fiebich BL, Goldsteins G, Keinanen R, Koistinaho J. Minocycline, a tetracycline derivative, is neuroprotective against excitotoxicity by inhibiting activation and proliferation of microglia. J Neurosci. 2001;21:2580–8.
68. Reis DJ, Casteen EJ, Ilardi SS. The antidepressant impact of minocycline in rodents: a systematic review and meta-analysis. Sci Rep. 2019;9:261.
69. Rosenblat JD, McIntyre RS. Efficacy and tolerability of minocycline for depression: a systematic review and meta-analysis of clinical trials. J Affect Disord. 2018;227:219–25.
70. Han Y, Zhang L, Wang Q, Zhang D, Zhao Q, Zhang J, et al. Minocycline inhibits microglial activation and alleviates depressive-like behaviors in male adolescent mice subjected to maternal separation. Psychoneuroendocrinology. 2019;107:37–45.
71. Rotheneichner P, Lange S, O'Sullivan A, Marschallinger J, Zaunmair P, Geretsegger C, et al. Hippocampal neurogenesis and antidepressive therapy: shocking relations. Neural Plast. 2014;2014:723915.
72. Brooks AK, Lawson MA, Smith RA, Janda TM, Kelley KW, McCusker RH. Interactions between inflammatory mediators and corticosteroids regulate transcription of genes within the Kynurenine Pathway in the mouse hippocampus. J Neuroinflamm. 2016;13:16.
73. Miller CL, Llenos IC, Dulay JR, Weis S. Upregulation of the initiating step of the kynurenine pathway in postmortem anterior cingulate cortex from individuals with schizophrenia and bipolar disorder. Brain Res. 2006;1073:25–37.
74. Ogura Y, Parsons WH, Kamat SS, Cravatt BF. A calcium-dependent acyltransferase that produces N-acyl phosphatidylethanolamines. Nat Chem Biol. 2016;12:669.
75. Haslinger A, Schwarz TJ, Covic M, Lie DC. Expression of Sox11 in adult neurogenic niches suggests a stage-specific role in adult neurogenesis. Eur J Neurosci. 2009;29:2103–14.
76. Takamura N, Nakagawa S, Masuda T, Boku S, Kato A, Song N, et al. The effect of dopamine on adult hippocampal neurogenesis. Prog Neuro-Psychopharmacol Biol Psychiatry. 2014;50:116–24.
77. Rossato JI, Bevilaqua LRM, Izquierdo I, Medina JH, Cammarota M. Dopamine Controls Persistence of Long-Term Memory Storage. Science. 2009;325:1017–20.
78. Kreisel T, Wolf B, Keshet E, Licht T. Unique role for dentate gyrus microglia in neuroblast survival and in VEGF-induced activation. Glia. 2019;67:594–618.
79. Hickman SE, Kingery ND, Ohsumi TK, Borowsky ML, Wang LC, Means TK, et al. The microglial sensome revealed by direct RNA sequencing. Nat Neurosci. 2013;16:1896–905.
80. Zhang Y, Chen K, Sloan SA, Bennett ML, Scholze AR, O'Keeffe S, et al. An RNA-sequencing transcriptome and splicing database of glia, neurons, and vascular cells of the cerebral cortex. J Neurosci. 2014;34:11929–47.
81. Galatro TF, Holtman IR, Lerario AM, Vainchtein ID, Brouwer N, Sola PR, et al. Transcriptomic analysis of purified human cortical microglia reveals age-associated changes. Nat Neurosci. 2017;20:1162.
82. Workman CJ, Vignali DA. The CD4-related molecule, LAG-3 (CD223), regulates the expansion of activated T cells. Eur J Immunol. 2003;33:970–9.
83. Goldberg MV, Drake CG. LAG-3 in cancer immunotherapy. Curr Top Microbiol Immunol. 2011;344:269–78.
84. Deczkowska A, Amit I, Schwartz M. Microglial immune checkpoint mechanisms. Nat Neurosci. 2018;21:779–86.
85. Parkhurst CN, Yang G, Ninan I, Savas JN, Yates JR 3rd, Lafaille JJ, et al. Microglia promote learning-dependent synapse formation through brain-derived neurotrophic factor. Cell. 2013;155:1596–609.

86. Reshef R, Kreisel T, Beroukhim Kay D, Yirmiya R. Microglia and their CX3CR1 signaling are involved in hippocampal- but not olfactory bulb-related memory and neurogenesis. Brain Behav Immun. 2014;41:239–50.
87. Ziv Y, Ron N, Butovsky O, Landa G, Sudai E, Greenberg N, et al. Immune cells contribute to the maintenance of neurogenesis and spatial learning abilities in adulthood. Nat Neurosci. 2006;9:268–75.
88. Sierra A, Tremblay ME, Wake H. Never-resting microglia: physiological roles in the healthy brain and pathological implications. Front Cell Neurosci. 2014;8:240.
89. Rice RA, Spangenberg EE, Yamate-Morgan H, Lee RJ, Arora RP, Hernandez MX, et al. Elimination of microglia improves functional outcomes following extensive neuronal loss in the hippocampus. J Neurosci. 2015;35:9977–89.
90. Elmore MR, Najafi AR, Koike MA, Dagher NN, Spangenberg EE, Rice RA, et al. Colony-stimulating factor 1 receptor signaling is necessary for microglia viability, unmasking a microglia progenitor cell in the adult brain. Neuron. 2014;82:380–97.
91. Walter TJ, Crews FT. Microglial depletion alters the brain neuroimmune response to acute binge ethanol withdrawal. J Neuroinflammation. 2017;14:86.
92. Yang X, Ren H, Wood K, Li M, Qiu S, Shi FD, et al. Depletion of microglia augments the dopaminergic neurotoxicity of MPTP. FASEB J. 2018;32:3336–45.
93. Wahlund B, Piazza P, von Rosen D, Liberg B, Liljenström H. Seizure (Ictal)-EEG characteristics in subgroups of depressive disorder in patients receiving electroconvulsive therapy (ECT)-a preliminary study and multivariate approach. Comput Intell Neurosci. 2009;965209.
94. Iaccarino HF, Singer AC, Martorell AJ, Rudenko A, Gao F, Gillingham TZ, et al. Gamma frequency entrainment attenuates amyloid load and modifies microglia. Nature. 2016;540:230–5.
95. Martorell AJ, Paulson AL, Suk HJ, Abdurrob F, Drummond GT, Guan W, et al. Multi-sensory gamma stimulation ameliorates alzheimer's-associated pathology and improves cognition. Cell. 2019;177:256–71 e222.
96. Xia J, Lu Z, Feng S, Yang J, Ji M. Different effects of immune stimulation on chronic unpredictable mild stress-induced anxiety- and depression-like behaviors depending on timing of stimulation. Int Immunopharmacol. 2018;58:48–56.
97. Kreisel T, Wolf B, Keshet E, Licht T. Unique role for dentate gyrus microglia in neuroblast survival and in VEGF-induced activation. Glia. 2018;67:594–618.
98. Mao XB, Ou MT, Karuppagounder SS, Kam TI, Yin XL, Xiong YL, et al. Pathological alpha-synuclein transmission initiated by binding lymphocyte-activation gene 3. Science. 2016;353:12.
99. Graydon CG, Mohideen S, Fowke KR. LAG3's enigmatic mechanism of action. Front Immunol. 2020;11:615317.
100. Triebel F. LAG-3: a regulator of T-cell and DC responses and its use in therapeutic vaccination. Trends Immunol. 2003;24:619–22.
101. Blackburn SD, Shin H, Haining WN, Zou T, Workman CJ, Polley A, et al. Coregulation of CD8+ T cell exhaustion by multiple inhibitory receptors during chronic viral infection. Nat Immunol. 2009;10:29–37.
102. Rexach JE, Polioudakis D, Yin A, Swarup V, Chang TS, Nguyen T, et al. Tau Pathology Drives Dementia Risk-Associated Gene Networks toward Chronic Inflammatory States and Immunosuppression. Cell Rep. 2020;33:108398.
103. Buisson S, Triebel F. LAG-3 (CD223) reduces macrophage and dendritic cell differentiation from monocyte precursors. Immunology. 2005;114:369–74.
104. Atwal JK, Chen Y, Chiu C, Mortensen DL, Meilandt WJ, Liu Y, et al. A therapeutic antibody targeting BACE1 inhibits amyloid-beta production in vivo. Sci Transl Med. 2011;3:84ra43.
105. Reiber H, Felgenhauer K. Protein transfer at the blood cerebrospinal fluid barrier and the quantitation of the humoral immune response within the central nervous system. Clin Chim Acta. 1987;163:319–28.
106. Menard C, Pfau ML, Hodes GE, Kana V, Wang VX, Bouchard S, et al. Social stress induces neurovascular pathology promoting depression. Nat Neurosci. 2017;20:1752–60.
107. Friedman A, Kaufer D, Shemer J, Hendler I, Soreq H, Tur-Kaspa I. Pyridostigmine brain penetration under stress enhances neuronal excitability and induces early immediate transcriptional response. Nat Med. 1996;2:1382–5.
108. Greene C, Hanley N, Campbell M. Blood-brain barrier associated tight junction disruption is a hallmark feature of major psychiatric disorders. Transl Psychiatry. 2020;10:373.
109. Niklasson F, Agren H. Brain energy metabolism and blood-brain barrier permeability in depressive patients: analyses of creatine, creatinine, urate, and albumin in CSF and blood. Biol Psychiatry. 1984;19:1183–206.
110. Kealy J, Greene C, Campbell M. Blood-brain barrier regulation in psychiatric disorders. Neurosci Lett. 2020;726:133664.
111. Wohleb ES, Powell ND, Godbout JP, Sheridan JF. Stress-induced recruitment of bone marrow-derived monocytes to the brain promotes anxiety-like behavior. J Neurosci. 2013;33:13820–33.
112. Grassivaro F, Menon R, Acquaviva M, Ottoboni L, Ruffini F, Bergamaschi A, et al. Convergence between microglia and peripheral macrophages phenotype during development and neuroinflammation. J Neurosci. 2020;40:784–95.
113. Olson JK, Miller SD. Microglia initiate central nervous system innate and adaptive immune responses through multiple TLRs. J Immunol. 2004;173:3916–24.
114. Horikawa H, Kato TA, Mizoguchi Y, Monji A, Seki Y, Ohkuri T, et al. Inhibitory effects of SSRIs on IFN-gamma induced microglial activation through the regulation of intracellular calcium. Prog Neuropsychopharmacol Biol Psychiatry. 2010;34:1306–16.
115. Hashioka S, Klegeris A, Monji A, Kato T, Sawada M, McGeer PL, et al. Antidepressants inhibit interferon-gamma-induced microglial production of IL-6 and nitric oxide. Exp Neurol. 2007;206:33–42.
116. Alboni S, Poggini S, Garofalo S, Milior G, El Hajj H, Lecours C, et al. Fluoxetine treatment affects the inflammatory response and microglial function according to the quality of the living environment. Brain Behav Immun. 2016;58:261–71.
117. Hinwood M, Tynan RJ, Charnley JL, Beynon SB, Day TA, Walker FR. Chronic stress induced remodeling of the prefrontal cortex: structural re-organization of microglia and the inhibitory effect of minocycline. Cereb Cortex. 2012;23:1784–97.
118. Rimmerman N, Juknat A, Kozela E, Levy R, Bradshaw HB, Vogel Z. The nonpsychoactive plant cannabinoid, cannabidiol affects cholesterol metabolism-related genes in microglial cells. Cell Mol Neurobiol. 2011;31:921–30.

ACKNOWLEDGEMENTS

We thank Ms. Zehava Cohen for help in preparation of the figures. We thank Dr. Gilgi Friedlander from the Nancy & Stephen Grand Israel National Center for Personalized Medicine (G-INCPM) for help with RNA-Seq and analysis. Postmortem brain tissue was donated by The Stanley Medical Research Institute brain collection. This research was supported by the Israel Science Foundation grant No. 1379/16 (to RY).

AUTHOR CONTRIBUTIONS

NR and RY designed and directed the studies. HV, HG, LN, ER, EK RR, LA, SG, RR, EA, NS, LBH, CP, MA, ED, and KL performed the experiments. NR, HV, HG, LN, EK RR, KMR, DMM, ABZ, and RY analyzed the data. RY designed the concept and obtained funding. NR and RY wrote the manuscript.

COMPETING INTERESTS

D.M.M. has received speaker's honoraria from MECTA and Otsuka and an honorarium from Janssen for participating in an esketamine advisory board meeting. The other authors declare no competing financial interests in relation to the work in this paper.

ADDITIONAL INFORMATION

Supplementary information The online version contains supplementary material available at https://doi.org/10.1038/s41380-021-01338-0.

Correspondence and requests for materials should be addressed to Raz Yirmiya.

Reprints and permission information is available at http://www.nature.com/reprints

Publisher's note Springer Nature remains neutral with regard to jurisdictional claims in published maps and institutional affiliations.